J. Fluid Mech. (2008), *vol.* 611, *pp.* 255–282. © 2008 Cambridge University Press
doi:10.1017/S0022112008002802 Printed in the United Kingdom

Transverse instability of interfacial solitary waves

TAKESHI KATAOKA

Department of Mechanical Engineering, Graduate School of Engineering, Kobe University, Rokkodai, Nada, Kobe 657-8501, Japan
kataoka@mech.kobe-u.ac.jp

(Received 4 July 2007 and in revised form 27 May 2008)

The linear stability of finite-amplitude interfacial solitary waves in a two-layer fluid of finite depth is examined analytically on the basis of the Euler equations. An asymptotic analysis is performed, which provides an explicit criterion of instability in the case of long-wavelength transverse disturbances. This result leads to the general statement that, when the amplitude of the solitary wave is increased, the solution becomes transversely unstable before an exchange of longitudinal stability occurs.

1. Introduction

Longitudinal stability is a stability to disturbances that depend only on the main wave travelling direction, while transverse stability is a stability to disturbances that depend also on its transverse direction. In the present paper, the transverse stability of finite-amplitude interfacial solitary waves in a two-layer fluid of finite depth is examined. The effect of interfacial tension is neglected. The corresponding small-amplitude solitary waves are known to be stable both longitudinally and transversely from analyses based on the Korteweg–de Vries (KdV) equation (Jeffery & Kakutani 1970; Benjamin 1972) and the Kadomtsev–Petviashvili (KP) equation with negative dispersion (Kadomtsev & Petviashvili 1970; Zakharov 1975).

In previous studies on the stability of finite-amplitude waves, surface solitary waves have been the main focus. Tanaka (1986) first examined their longitudinal stability on the basis of the Euler equations, and discovered that an exchange of longitudinal stability occurs at the first stationary value of the total wave energy. The corresponding maximum surface displacement is 0.781 times the undisturbed depth of the fluid. Tanaka *et al.* (1987) also conducted numerical simulations to study the time development of a disturbed surface solitary wave, and found that the growth rate of sufficiently small disturbance agrees well with that of the linear stability analysis. A more precise linear stability analysis was carried out later by Longuet-Higgins & Tanaka (1997).

The transverse stability of surface solitary waves was examined by Kataoka & Tsutahara (2004*a*). The criterion of transverse instability is derived analytically, and it is found that the surface solitary waves are transversely unstable if the maximum surface displacement is greater than 0.713 times the undisturbed depth of the fluid. This critical amplitude is well below that (= 0.781) for the longitudinal instability. Thus, the stability of surface solitary waves has been clarified to some extent.

For finite-amplitude interfacial solitary waves (with no interfacial tension effects), on the other hand, it is only recently that the study of their stability has been initiated (see Calvo & Akylas 2003 for the case of strong interfacial tension effects). The present author examined their longitudinal stability analytically on the basis of the

https://doi.org/10.1017/S0022112008002802 Published online by Cambridge University Press

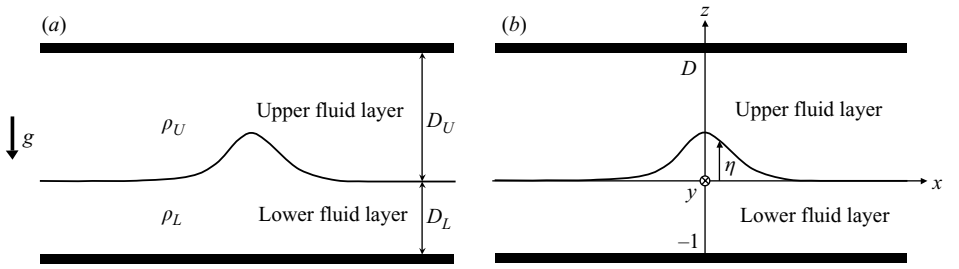


FIGURE 1. Geometry: (*a*) dimensional system; (*b*) non-dimensional system.

Euler equations (Kataoka 2006), and found that an exchange of longitudinal stability occurs at every stationary value of the total wave energy. There are no previous studies on the transverse stability, however, as far as the author knows, and it is treated in the present work. Since the number of parameters of interfacial solitary waves is three (due to the addition of the density ratio and the depth ratio of the two layers) instead of one for surface solitary waves, it is an enormous task even to gain a general view from numerical stability analysis. It is, therefore, desirable to derive a stability criterion not numerically but analytically. Following the analytical method used in Kataoka & Tsutahara (2004*a*), we here examine the linear stability with respect to long-wavelength transverse disturbances. We then obtain a sufficient condition for the transverse instability explicitly, which leads to the general statement that, when the branch of the solitary wave solution is traced from small amplitude, the solution becomes transversely unstable before an exchange of longitudinal stability occurs.

In § 2 we formulate basic equations. The stability problem is reduced to a linear eigenvalue problem. In § 3, we solve this eigenvalue problem for small transverse wavenumbers of disturbances, and obtain a criterion of transverse instability. In § 4 this criterion is used to derive a general statement on the stability of interfacial solitary waves, and in § 5 we apply the criterion to various solitary wave solutions to study their transverse instability specifically. In § 6, the analytical solution obtained in § 3 is physically interpreted, and finally in § 7 some concluding remarks follow.

2. Basic equations

Consider a two-layer fluid where a lighter fluid lies above a heavier fluid under uniform acceleration due to gravity g (see figure 1*a*). The density of the upper fluid is ρ_U and that of the lower $\rho_L(>\rho_U)$. The fluids are incompressible, inviscid, and occupy a channel between two horizontal rigid boundaries where the upper fluid layer has undisturbed depth D_U and the lower layer D_L. In what follows, index U refers to the upper fluid and index L to the lower, and all variables are non-dimensionalized using g, ρ_L, and D_L. The flow in each layer is irrotational and the effect of interfacial tension is neglected. Let x, y, z be the Cartesian coordinates with the z-axis pointing vertically upward and the origin located on the undisturbed interface (see figure 1*b*). The fluid motion is governed by

$$\frac{\partial^2\phi_U}{\partial x^2}+\frac{\partial^2\phi_U}{\partial y^2}+\frac{\partial^2\phi_U}{\partial z^2}=0 \quad \text{for } \eta<z<D, \tag{2.1}$$

https://doi.org/10.1017/S0022112008002802 Published online by Cambridge University Press

$$\frac{\partial^2\phi_L}{\partial x^2}+\frac{\partial^2\phi_L}{\partial y^2}+\frac{\partial^2\phi_L}{\partial z^2}=0 \quad \text{for} \quad -1<z<\eta, \tag{2.2}$$

$$\frac{\partial\phi_U}{\partial z}=0 \quad \text{at} \quad z=D, \tag{2.3}$$

$$\frac{\partial\eta}{\partial t}+\frac{\partial\phi_U}{\partial x}\frac{\partial\eta}{\partial x}+\frac{\partial\phi_U}{\partial y}\frac{\partial\eta}{\partial y}=\frac{\partial\phi_U}{\partial z} \quad \text{at} \quad z=\eta, \tag{2.4}$$

$$\frac{\partial\eta}{\partial t}+\frac{\partial\phi_L}{\partial x}\frac{\partial\eta}{\partial x}+\frac{\partial\phi_L}{\partial y}\frac{\partial\eta}{\partial y}=\frac{\partial\phi_L}{\partial z} \quad \text{at} \quad z=\eta, \tag{2.5}$$

$$\begin{aligned}&-\rho\left\{\frac{\partial\phi_U}{\partial t}+\frac{1}{2}\left[\left(\frac{\partial\phi_U}{\partial x}\right)^2+\left(\frac{\partial\phi_U}{\partial y}\right)^2+\left(\frac{\partial\phi_U}{\partial z}\right)^2\right]\right\}+\frac{\partial\phi_L}{\partial t}\\&+\frac{1}{2}\left[\left(\frac{\partial\phi_L}{\partial x}\right)^2+\left(\frac{\partial\phi_L}{\partial y}\right)^2+\left(\frac{\partial\phi_L}{\partial z}\right)^2\right]+(1-\rho)\eta=f(t) \quad \text{at} \quad z=\eta,\end{aligned} \tag{2.6}$$

$$\frac{\partial\phi_L}{\partial z}=0 \quad \text{at} \quad z=-1, \tag{2.7}$$

where t is the time, $\phi_U(x, y, z, t)$ and $\phi_L(x, y, z, t)$ are the velocity potentials of the upper and lower fluids, respectively, $\eta(x, y, t)$ is the interfacial elevation, and $f(t)$ is a given function of t. The ρ and D are, respectively, the density ratio and the depth ratio of the two fluids defined by

$$\rho=\frac{\rho_U}{\rho_L}, \quad D=\frac{D_U}{D_L}. \tag{2.8}$$

The cases $0\leqslant\rho<1$ (statically stable) and $0<D<\infty$ (finite depth) are considered throughout this paper.

Let us consider a solution of (2.1)–(2.7) which is independent of t and y in the following form:

$$\phi_U=-vx+\Phi_U(x, z; v), \quad \phi_L=-vx+\Phi_L(x, z; v), \quad \eta=\eta_I(x; v), \tag{2.9}$$

with

$$f(t)=(1-\rho)v^2/2, \tag{2.10}$$

where v is a positive real parameter, and $\partial\Phi_U/\partial x$, $\partial\Phi_U/\partial z$, $\partial\Phi_L/\partial x$, $\partial\Phi_L/\partial z$, and η_I decay as $x\to\pm\infty$. Φ_U, Φ_L, and η_I are governed by

$$\nabla_2^2\Phi_U=0 \quad \text{for} \quad \eta<z<D, \tag{2.11}$$

$$\nabla_2^2\Phi_L=0 \quad \text{for} \quad -1<z<\eta, \tag{2.12}$$

$$\frac{\partial\Phi_U}{\partial z}=0 \quad \text{at} \quad z=D, \tag{2.13}$$

$$\left(-v+\frac{\partial\Phi_U}{\partial x}\right)\frac{\mathrm{d}\eta_I}{\mathrm{d}x}=\frac{\partial\Phi_U}{\partial z} \quad \text{at} \quad z=\eta_I, \tag{2.14}$$

$$\left(-v+\frac{\partial\Phi_L}{\partial x}\right)\frac{\mathrm{d}\eta_I}{\mathrm{d}x}=\frac{\partial\Phi_L}{\partial z} \quad \text{at} \quad z=\eta_I, \tag{2.15}$$

https://doi.org/10.1017/S0022112008002802 Published online by Cambridge University Press

$$\rho v\frac{\partial \Phi_U}{\partial x}-\frac{\rho}{2}\left[\left(\frac{\partial \Phi_U}{\partial x}\right)^2+\left(\frac{\partial \Phi_U}{\partial z}\right)^2\right]-v\frac{\partial \Phi_L}{\partial x}$$
$$+\frac{1}{2}\left[\left(\frac{\partial \Phi_L}{\partial x}\right)^2+\left(\frac{\partial \Phi_L}{\partial z}\right)^2\right]+(1-\rho)\eta_I=0 \quad \text{at} \quad z=\eta_I, \tag{2.16}$$

$$\frac{\partial \Phi_L}{\partial z}=0 \quad \text{at} \quad z=-1, \tag{2.17}$$

$$\frac{\partial \Phi_U}{\partial x}\to 0, \quad \frac{\partial \Phi_U}{\partial z}\to 0, \quad \frac{\partial \Phi_L}{\partial x}\to 0, \quad \frac{\partial \Phi_L}{\partial z}\to 0, \quad \eta_I\to 0 \quad \text{as} \quad x\to\pm\infty, \tag{2.18}$$

where

$$\nabla_2^2=\frac{\partial^2}{\partial x^2}+\frac{\partial^2}{\partial z^2}. \tag{2.19}$$

The solution (2.9) represents a steady propagation of two-dimensional localized wave against a uniform stream of constant velocity $-v$ in the x-direction. When the solution exists, the decay described in (2.18) is exponentially fast, and the origin of the x-coordinate can be chosen such that $\partial\Phi_U/\partial x$, $\partial\Phi_L/\partial x$, and η_I are even in x. We call this solution a solitary wave solution. The existence of the solitary wave solution has been confirmed both analytically and numerically for various sets of the parameters ρ, D, and v (Amick & Turner 1986; Funakoshi & Oikawa 1986; Pullin & Grimshaw 1988; Turner & Vanden-Broeck 1988; Evans & Ford 1996; Laget & Dias 1997; Michallet & Barthélemy 1998; Grue *et al.* 1999; Kataoka 2006). According to the previous studies and the results of our numerical computation (part of which is shown in §4 below), the condition for the existence of the solitary wave solution is

$$c<v<V, \tag{2.20}$$

where

$$c=\sqrt{\frac{1-\rho}{1+\rho/D}} \tag{2.21}$$

is the phase speed of a linear long non-dispersive wave, and V is specifically given as follows:

(i) When ρ is larger than some critical value, or $\rho>\rho_{\rm cr}(D)$, where $\rho_{\rm cr}(D)$ is an increasing function of D, e.g.

$$\rho_{\rm cr}(D)=\begin{cases}0.0005\sim 0.0006 \text{ at } D=1,\\ 0.05\sim 0.06 \text{ at } D=3,\\ 0.19\sim 0.21 \text{ at } D=10,\end{cases} \tag{2.22}$$

V is equal to the propagation speed of internal bores:

$$V=\sqrt{\frac{(D+1)(1-\sqrt{\rho})}{1+\sqrt{\rho}}} \quad \text{for } \rho>\rho_{\rm cr}(D) \tag{2.23}$$

(Funakoshi & Oikawa 1986; Laget & Dias 1997; Dias & Vanden-Broeck 2003).

https://doi.org/10.1017/S0022112008002802 Published online by Cambridge University Press

(ii) When ρ is smaller than the above critical value, or $\rho < \rho_{\rm cr}(D)$, V is smaller than the propagation speed of internal bores:

$$V < \sqrt{\frac{(D+1)(1-\sqrt{\rho})}{1+\sqrt{\rho}}} \quad \text{for} \quad \rho < \rho_{\rm cr}(D), \tag{2.24}$$

and a precise upper limiting value V in this case is not found due to the computational difficulty in specifying it.

In order to examine the linear stability of the above solitary wave solution (2.9) on the basis of (2.1)–(2.7), the following form is assumed for a solution of (2.1)–(2.7):

$$\phi_U = -vx + \Phi_U + \hat{\phi}_U(x,z)\exp(\lambda t + {\rm i}\varepsilon y), \tag{2.25a}$$

$$\phi_L = -vx + \Phi_L + \hat{\phi}_L(x,z)\exp(\lambda t + {\rm i}\varepsilon y), \tag{2.25b}$$

$$\eta = \eta_I + \hat{\eta}(x)\exp(\lambda t + {\rm i}\varepsilon y), \tag{2.25c}$$

where ε is a given positive constant and λ is a complex constant to be determined. Substituting (2.25) into (2.1)–(2.7) and linearizing with respect to $(\hat{\phi}_U, \hat{\phi}_L, \hat{\eta})$, we obtain the eigenvalue problem which has eigenvalue λ. If there exists a solution $(\hat{\phi}_U, \hat{\phi}_L, \hat{\eta})$ for which λ has a positive real part, the corresponding solitary wave is linearly unstable. The longitudinal stability, or the stability with respect to disturbances that have no dependence on y ($\varepsilon = 0$) was examined analytically in Kataoka (2006). It was found that an exchange of longitudinal stability (the appearance of a positive real eigenvalue λ from zero) occurs at the stationary value (or ${\rm d}E/{\rm d}v = 0$) of the total energy E of the solitary wave defined by

$$E(v) = \int_{-\infty}^{\infty} \left\{ \frac{\rho}{2} \int_{\eta_I}^{D} \left[\left(\frac{\partial \Phi_U}{\partial x} \right)^2 + \left(\frac{\partial \Phi_U}{\partial z} \right)^2 \right] {\rm d}z + \frac{1}{2} \int_{-1}^{\eta_I} \left[\left(\frac{\partial \Phi_L}{\partial x} \right)^2 + \left(\frac{\partial \Phi_L}{\partial z} \right)^2 \right] {\rm d}z + \frac{1-\rho}{2} \eta_I^2 \right\} {\rm d}x, \tag{2.26}$$

and the eigenvalue λ of small modulus ($|\lambda| \ll 1$) near the stability threshold $|{\rm d}E/{\rm d}v| \ll 1$ is given by

$$\lambda = \begin{cases} \pm \left(v \dfrac{{\rm d}M}{{\rm d}v} \dfrac{{\rm d}\Omega}{{\rm d}v} \right)^{-1} \dfrac{{\rm d}E}{{\rm d}v} & \text{for } \dfrac{{\rm d}E}{{\rm d}v} \dfrac{{\rm d}M}{{\rm d}v} \dfrac{{\rm d}\Omega}{{\rm d}v} > 0, \\ \text{no real solution} & \text{for } \dfrac{{\rm d}E}{{\rm d}v} \dfrac{{\rm d}M}{{\rm d}v} \dfrac{{\rm d}\Omega}{{\rm d}v} < 0, \end{cases} \tag{2.27}$$

if the solitary wave solutions do not bifurcate and v never becomes stationary at the stationary value of E. Here Ω and M are properties of the solitary wave defined by

$$\Omega(v) = \frac{2}{v}\left(T_L - \frac{T_U}{D} \right) - \left(1 + \frac{\rho}{D} \right) vM, \quad M(v) = \int_{-\infty}^{\infty} \eta_I \, {\rm d}x, \tag{2.28a,b}$$

with

$$T_U(v) = \frac{\rho}{2} \int_{-\infty}^{\infty} {\rm d}x \int_{\eta_I}^{D} \left[\left(\frac{\partial \Phi_U}{\partial x} \right)^2 + \left(\frac{\partial \Phi_U}{\partial z} \right)^2 \right] {\rm d}z, \tag{2.28c}$$

$$T_L(v) = \frac{1}{2} \int_{-\infty}^{\infty} {\rm d}x \int_{-1}^{\eta_I} \left[\left(\frac{\partial \Phi_L}{\partial x} \right)^2 + \left(\frac{\partial \Phi_L}{\partial z} \right)^2 \right] {\rm d}z, \tag{2.28d}$$

where M represents the mass, and T_U and T_L are the kinetic energy in the upper and lower fluid layers, respectively.

https://doi.org/10.1017/S0022112008002802 Published online by Cambridge University Press

Now we investigate the transverse stability, or the stability with respect to disturbances that depend not only on the x- and z-directions but also on the y-direction ($\varepsilon > 0$). Substituting (2.25) into (2.1)–(2.7), linearizing with respect to $(\hat{\phi}_U, \hat{\phi}_L, \hat{\eta})$, and imposing decaying conditions as $x \to \pm\infty$, we obtain the following set of linear equations for $(\hat{\phi}_U, \hat{\phi}_L, \hat{\eta})$:

$$\nabla_2^2 \hat{\phi}_U = \varepsilon^2 \hat{\phi}_U \quad \text{for} \quad \eta_I < z < D, \tag{2.29}$$

$$\nabla_2^2 \hat{\phi}_L = \varepsilon^2 \hat{\phi}_L \quad \text{for} \quad -1 < z < \eta_I, \tag{2.30}$$

$$\frac{\partial \hat{\phi}_U}{\partial z} = 0 \quad \text{at} \quad z = D, \tag{2.31}$$

$$\mathrm{L_U}[\hat{\phi}_U, \hat{\eta}] = -\lambda \hat{\eta} \quad \text{at} \quad z = \eta_I, \tag{2.32}$$

$$\mathrm{L_L}[\hat{\phi}_L, \hat{\eta}] = -\lambda \hat{\eta} \quad \text{at} \quad z = \eta_I, \tag{2.33}$$

$$\mathrm{L_I}[\hat{\phi}_U, \hat{\phi}_L, \hat{\eta}] = \lambda(\rho \hat{\phi}_U - \hat{\phi}_L) \quad \text{at} \quad z = \eta_I, \tag{2.34}$$

$$\frac{\partial \hat{\phi}_L}{\partial z} = 0 \quad \text{at} \quad z = -1, \tag{2.35}$$

$$\hat{\phi}_U(x, z) \to 0, \quad \hat{\phi}_L(x, z) \to 0, \quad \hat{\eta}(x) \to 0 \quad \text{as} \quad x \to \pm\infty, \tag{2.36}$$

where ∇_2^2, $\mathrm{L_U}$, $\mathrm{L_L}$, and $\mathrm{L_I}$ are the linear operators defined by (2.19) and

$$\mathrm{L_U}[\hat{\phi}_U, \hat{\eta}] = \left(-\frac{\partial}{\partial z} + \frac{\mathrm{d}\eta_I}{\mathrm{d}x}\frac{\partial}{\partial x}\right)\hat{\phi}_U + \left[\left(\frac{\partial^2 \Phi_U}{\partial x^2} + \frac{\partial^2 \Phi_U}{\partial x \partial z}\frac{\mathrm{d}\eta_I}{\mathrm{d}x}\right) + \left(-v + \frac{\partial \Phi_U}{\partial x}\right)\frac{\mathrm{d}}{\mathrm{d}x}\right]\hat{\eta}, \tag{2.37}$$

$$\mathrm{L_L}[\hat{\phi}_L, \hat{\eta}] = \left(-\frac{\partial}{\partial z} + \frac{\mathrm{d}\eta_I}{\mathrm{d}x}\frac{\partial}{\partial x}\right)\hat{\phi}_L + \left[\left(\frac{\partial^2 \Phi_L}{\partial x^2} + \frac{\partial^2 \Phi_L}{\partial x \partial z}\frac{\mathrm{d}\eta_I}{\mathrm{d}x}\right) + \left(-v + \frac{\partial \Phi_L}{\partial x}\right)\frac{\mathrm{d}}{\mathrm{d}x}\right]\hat{\eta}, \tag{2.38}$$

$$\begin{aligned}\mathrm{L_I}[\hat{\phi}_U, \hat{\phi}_L, \hat{\eta}] = &-\rho\left[\left(-v + \frac{\partial \Phi_U}{\partial x}\right)\frac{\partial}{\partial x} + \frac{\partial \Phi_U}{\partial z}\frac{\partial}{\partial z}\right]\hat{\phi}_U \\ &+\left[\left(-v + \frac{\partial \Phi_L}{\partial x}\right)\frac{\partial}{\partial x} + \frac{\partial \Phi_L}{\partial z}\frac{\partial}{\partial z}\right]\hat{\phi}_L \\ &+\left\{-\rho\left[\left(-v + \frac{\partial \Phi_U}{\partial x}\right)\frac{\partial^2 \Phi_U}{\partial x \partial z} + \frac{\partial \Phi_U}{\partial z}\frac{\partial^2 \Phi_U}{\partial z^2}\right]\right. \\ &\left.+\left(-v + \frac{\partial \Phi_L}{\partial x}\right)\frac{\partial^2 \Phi_L}{\partial x \partial z} + \frac{\partial \Phi_L}{\partial z}\frac{\partial^2 \Phi_L}{\partial z^2} + 1 - \rho\right\}\hat{\eta}.\end{aligned} \tag{2.39}$$

Equations (2.29)–(2.36) constitute an eigenvalue problem for $(\hat{\phi}_U, \hat{\phi}_L, \hat{\eta})$ with eigenvalue λ. In the next section we solve this eigenvalue problem (2.29)–(2.36) for small ε in order to study the stability of the solitary wave to long-wavelength transverse disturbances.

3. Stability to long-wavelength transverse disturbances

We seek an asymptotic solution of (2.29)–(2.36) for small ε. At leading order in ε, the terms on the right-hand sides of (2.29) and (2.30) can be ignored, and the

https://doi.org/10.1017/S0022112008002802 Published online by Cambridge University Press

eigenvalue problem (2.29)–(2.36) has the following leading-order solution with $\lambda = 0$:

$$\hat{\phi}_U = \hat{\phi}_{UC}^{(0)} \equiv \frac{\partial \Phi_U}{\partial x}, \quad \hat{\phi}_L = \hat{\phi}_{LC}^{(0)} \equiv \frac{\partial \Phi_L}{\partial x}, \quad \hat{\eta} = \hat{\eta}_C^{(0)} \equiv \frac{\mathrm{d}\eta_I}{\mathrm{d}x}, \quad \lambda = 0. \tag{3.1}$$

The λ will be non-zero if the terms on the right-hand sides of (2.29) and (2.30), or the terms of $O(\varepsilon^2)$ are recovered. Since the recovered terms are $O(\varepsilon^2)$, we may conjecture that $\lambda = O(\varepsilon^2)$. However, this is only a rough estimate and in the analysis we impose a weaker condition that $\lambda = O(\varepsilon)$, i.e.

$$\lambda = \varepsilon\lambda_1 + \varepsilon^2\lambda_2 + \cdots, \tag{3.2}$$

where λ_n $(n = 1, 2, \ldots)$ is a complex constant to be determined.† The above choice of the weaker condition (3.2) on λ is, in fact, essential for consistency of the following analysis.

Let us look for a solution $(\hat{\phi}_U, \hat{\phi}_L, \hat{\eta})$ of (2.29)–(2.35) with a moderate variation in x and z ($\partial\hat{h}/\partial x = O(\hat{h})$ and $\partial\hat{h}/\partial z = O(\hat{h})$, where $\hat{h}$ represents $(\hat{\phi}_U, \hat{\phi}_L, \hat{\eta})$), in the following power series of ε:

$$\hat{\phi}_{UC} = \hat{\phi}_{UC}^{(0)} + \varepsilon\hat{\phi}_{UC}^{(1)} + \varepsilon^2\hat{\phi}_{UC}^{(2)} + \cdots, \tag{3.3a}$$

$$\hat{\phi}_{LC} = \hat{\phi}_{LC}^{(0)} + \varepsilon\hat{\phi}_{LC}^{(1)} + \varepsilon^2\hat{\phi}_{LC}^{(2)} + \cdots, \tag{3.3b}$$

$$\hat{\eta}_C = \hat{\eta}_C^{(0)} + \varepsilon\hat{\eta}_C^{(1)} + \varepsilon^2\hat{\eta}_C^{(2)} + \cdots, \tag{3.3c}$$

where the subscript C is attached to indicate the type of solution (core solution).

Substituting (3.2) and (3.3) into (2.29)–(2.35) and collecting the same-order terms in ε, we obtain a series of equations for $(\hat{\phi}_{UC}^{(n)}, \hat{\phi}_{LC}^{(n)}, \hat{\eta}_C^{(n)})$ $(n = 1, 2, \ldots)$:

$$\nabla_2^2\hat{\phi}_{UC}^{(n)} = \hat{\phi}_{UC}^{(n-2)} \quad \text{for } \eta_I < z < D, \tag{3.4}$$

$$\nabla_2^2\hat{\phi}_{LC}^{(n)} = \hat{\phi}_{LC}^{(n-2)} \quad \text{for } -1 < z < \eta_I, \tag{3.5}$$

$$\frac{\partial\hat{\phi}_{UC}^{(n)}}{\partial z} = 0 \quad \text{at} \quad z = D, \tag{3.6}$$

$$\mathrm{L_U}\left[\hat{\phi}_{UC}^{(n)}, \hat{\eta}_C^{(n)}\right] = G^{(n)} \quad \text{at} \quad z = \eta_I, \tag{3.7}$$

$$\mathrm{L_L}\left[\hat{\phi}_{LC}^{(n)}, \hat{\eta}_C^{(n)}\right] = G^{(n)} \quad \text{at} \quad z = \eta_I, \tag{3.8}$$

$$\mathrm{L_I}\left[\hat{\phi}_{UC}^{(n)}, \hat{\phi}_{LC}^{(n)}, \hat{\eta}_C^{(n)}\right] = H^{(n)} \quad \text{at} \quad z = \eta_I, \tag{3.9}$$

$$\frac{\partial\hat{\phi}_{LC}^{(n)}}{\partial z} = 0 \quad \text{at} \quad z = -1, \tag{3.10}$$

where $\hat{\phi}_{UC}^{(-1)} = \hat{\phi}_{LC}^{(-1)} = 0$ and

$$G^{(n)} = -\sum_{m=1}^{n}\lambda_m\hat{\eta}_C^{(n-m)} = \begin{cases} -\lambda_1\hat{\eta}_C^{(0)} & (n = 1), \\ -\lambda_1\hat{\eta}_C^{(1)} - \lambda_2\hat{\eta}_C^{(0)} & (n = 2), \\ \cdots, \end{cases} \tag{3.11}$$

† The stability of the solitary wave is determined at $\lambda = O(\varepsilon)$ or $O(\varepsilon^2)$ because the terms of $O(\varepsilon^2)$ appear in the basic equations (2.29) and (2.30). The λ is, however, expanded up to an infinite order in (3.2) because the higher-order terms of $O(\varepsilon^3)$ are *a priori* non-zero. However, these higher-order terms have no influence on the stability.

https://doi.org/10.1017/S0022112008002802 Published online by Cambridge University Press

$$H^{(n)}=\sum_{m=1}^{n}\lambda_m\big(\rho\hat{\phi}_{UC}^{(n-m)}-\hat{\phi}_{LC}^{(n-m)}\big)=\begin{cases}\lambda_1\big(\rho\hat{\phi}_{UC}^{(0)}-\hat{\phi}_{LC}^{(0)}\big) & (n=1),\\ \lambda_1\big(\rho\hat{\phi}_{UC}^{(1)}-\hat{\phi}_{LC}^{(1)}\big)+\lambda_2\big(\rho\hat{\phi}_{UC}^{(0)}-\hat{\phi}_{LC}^{(0)}\big) & (n=2),\\ \cdots.\end{cases} \tag{3.12}$$

The above set of equations (3.4)–(3.10) is linear and inhomogeneous and its homogeneous part has a non-trivial solution (3.1) that decays exponentially as $x\to\pm\infty$. Therefore, for this set of equations (3.4)–(3.10) to have a solution that does not diverge exponentially as $x\to\pm\infty$, its inhomogeneous terms must satisfy the solvability condition. Since the homogeneous part satisfies

$$\int_{-\infty}^{\infty}\Bigg\{\int_{\eta_I}^{D}\rho\frac{\partial\Phi_U}{\partial x}\nabla_2^2\hat{\phi}_{UC}^{(n)}\,\mathrm{d}z+\int_{-1}^{\eta_I}\frac{\partial\Phi_L}{\partial x}\nabla_2^2\hat{\phi}_{LC}^{(n)}\,\mathrm{d}z$$
$$+\left[-\rho\frac{\partial\Phi_U}{\partial x}\mathrm{L_U}\big[\hat{\phi}_{UC}^{(n)},\hat{\eta}_C^{(n)}\big]+\frac{\partial\Phi_L}{\partial x}\mathrm{L_L}\big[\hat{\phi}_{LC}^{(n)},\hat{\eta}_C^{(n)}\big]-\frac{\mathrm{d}\eta_I}{\mathrm{d}x}\mathrm{L_I}\big[\hat{\phi}_{UC}^{(n)},\hat{\phi}_{LC}^{(n)},\hat{\eta}_C^{(n)}\big]\right]_{z=\eta_I}\Bigg\}\mathrm{d}x=0,$$

the corresponding inhomogeneous terms $\hat{\phi}_{UC}^{(n-2)}$, $\hat{\phi}_{LC}^{(n-2)}$, $G^{(n)}$, and $H^{(n)}$ on the right-hand sides of (3.4)–(3.10) must satisfy

$$\int_{-\infty}^{\infty}\left(\rho\int_{\eta_I}^{D}\frac{\partial\Phi_U}{\partial x}\hat{\phi}_{UC}^{(n-2)}\mathrm{d}z+\int_{-1}^{\eta_I}\frac{\partial\Phi_L}{\partial x}\hat{\phi}_{LC}^{(n-2)}\mathrm{d}z\right)\mathrm{d}x$$
$$+\int_{-\infty}^{\infty}\left[\left(-\rho\frac{\partial\Phi_U}{\partial x}+\frac{\partial\Phi_L}{\partial x}\right)G^{(n)}-\frac{\mathrm{d}\eta_I}{\mathrm{d}x}H^{(n)}\right]_{z=\eta_I}\mathrm{d}x=0, \tag{3.13}$$

where the quantities in the square brackets with subscript $z=\eta_I$ are evaluated at $z=\eta_I$.

For $n=1$, (3.13) is identically satisfied, and a solution of (3.4)–(3.10) is

$$\hat{\phi}_{UC}^{(1)}=-\lambda_1\frac{\partial\Phi_U}{\partial v},\quad \hat{\phi}_{LC}^{(1)}=-\lambda_1\frac{\partial\Phi_L}{\partial v},\quad \hat{\eta}_C^{(1)}=-\lambda_1\frac{\partial\eta_I}{\partial v}, \tag{3.14}$$

where $\partial\Phi_U/\partial v$, $\partial\Phi_L/\partial v$, and $\partial\eta_I/\partial v$ are the derivatives of Φ_U, Φ_L, and η_I with respect to v for fixed x and z. The homogeneous solution (3.1) multiplied by an arbitrary constant is omitted in (3.14) because it can be incorporated into the leading-order solution (3.1). The solution (3.14), however, does not satisfy the decaying boundary conditions (2.36), since $\partial\Phi_U/\partial v$ and $\partial\Phi_L/\partial v$ do not decay either as $x\to\infty$ or $x\to-\infty$. In fact, in order to construct a solution that satisfies (2.36), we also must seek a solution whose variation is slow in x. This solution will be called a far-field solution. By matching the present core solution (3.3) with the far-field solution, the overall solution of (2.29)–(2.35) that satisfies the boundary conditions (2.36) can be constructed. In this section we concentrate on obtaining the core solution putting aside the boundary conditions (2.36), while Appendices B and C contain the far-field solution and the matching, respectively.

For $n=2$, (3.13) becomes

$$\frac{\lambda_1^2}{v}\frac{\mathrm{d}E}{\mathrm{d}v}=-E, \tag{3.15}$$

where E is defined by (2.26), and use has been made of

$$\int_{-\infty}^{\infty}\left[\rho\int_{\eta_I}^{D}\left(\frac{\partial\Phi_U}{\partial x}\right)^2\mathrm{d}z+\int_{-1}^{\eta_I}\left(\frac{\partial\Phi_L}{\partial x}\right)^2\mathrm{d}z\right]\mathrm{d}x-E=0 \tag{3.16}$$

https://doi.org/10.1017/S0022112008002802 Published online by Cambridge University Press

(see Appendix A for a derivation). When (3.15) is satisfied, a solution of (3.4)–(3.10) for $n=2$ is

$$\hat{\phi}^{(2)}_{UC}=\bar{\phi}^{(2)}_{UC}-\lambda_2\frac{\partial \Phi_U}{\partial v},\quad \hat{\phi}^{(2)}_{LC}=\bar{\phi}^{(2)}_{LC}-\lambda_2\frac{\partial \Phi_L}{\partial v},\quad \hat{\eta}^{(2)}_{C}=\bar{\eta}^{(2)}_{C}-\lambda_2\frac{\partial \eta_I}{\partial v}, \tag{3.17}$$

where $(\bar{\phi}^{(2)}_{UC},\bar{\phi}^{(2)}_{LC},\bar{\eta}^{(2)}_{C})$ is a particular solution of (3.4)–(3.10) for $n=2$ whose inhomogeneous terms $G^{(2)}$ and $H^{(2)}$ are replaced by $-\lambda_1\hat{\eta}^{(1)}_C$ and $\lambda_1(\rho\hat{\phi}^{(1)}_{UC}-\hat{\phi}^{(1)}_{LC})$, respectively. From (3.15), we have

$$\lambda_1=\begin{cases}\pm\sqrt{\dfrac{-vE}{\mathrm{d}E/\mathrm{d}v}} & \text{for } \dfrac{\mathrm{d}E}{\mathrm{d}v}<0,\\[2ex] \pm\mathrm{i}\sqrt{\dfrac{vE}{\mathrm{d}E/\mathrm{d}v}} & \text{for } \dfrac{\mathrm{d}E}{\mathrm{d}v}>0.\end{cases} \tag{3.18}$$

When $\mathrm{d}E/\mathrm{d}v<0$, the solitary wave is transversely unstable, since there is a solution for which the eigenvalue has a positive real part. When $\mathrm{d}E/\mathrm{d}v>0$, the stability is not determined at this order, since the real part of λ_1 is zero. To find the stability in the latter case, we must proceed to the next order.

At $n=3$, (3.13) becomes

$$\frac{2\lambda_1\lambda_2}{v}\frac{\mathrm{d}E}{\mathrm{d}v}=\left[\rho\hat{\phi}^{(1)}_{UC}\hat{u}^{(2)}_{UC}-\hat{\phi}^{(1)}_{LC}\hat{u}^{(2)}_{LC}\right]_{x\to\infty}-\left[\rho\hat{\phi}^{(1)}_{UC}\hat{u}^{(2)}_{UC}-\hat{\phi}^{(1)}_{LC}\hat{u}^{(2)}_{LC}\right]_{x\to-\infty}, \tag{3.19}$$

where the quantities in the square brackets with subscript $x\to\infty$ or $x\to-\infty$ are evaluated as $x\to\infty$ or $x\to-\infty$, respectively, and

$$\begin{aligned}\hat{u}^{(2)}_{UC}&\equiv-\int_{\eta_I}^{D}\frac{\partial\hat{\phi}^{(2)}_{UC}}{\partial x}\,\mathrm{d}z+\left(-v+\left[\frac{\partial\Phi_U}{\partial x}\right]_{z=\eta_I}\right)\hat{\eta}^{(2)}_C\\&=\left[\hat{u}^{(2)}_{UC}\right]_{x\to\infty}-\lambda_2\eta_I+\int_{\infty}^{x}\left(-\int_{\eta_I}^{D}\frac{\partial\Phi_U}{\partial x}\,\mathrm{d}z+\lambda_1^2\frac{\partial\eta_I}{\partial v}\right)\mathrm{d}x',\end{aligned} \tag{3.20a}$$

$$\begin{aligned}\hat{u}^{(2)}_{LC}&\equiv\int_{-1}^{\eta_I}\frac{\partial\hat{\phi}^{(2)}_{LC}}{\partial x}\,\mathrm{d}z+\left(-v+\left[\frac{\partial\Phi_L}{\partial x}\right]_{z=\eta_I}\right)\hat{\eta}^{(2)}_C\\&=\left[\hat{u}^{(2)}_{LC}\right]_{x\to\infty}-\lambda_2\eta_I+\int_{\infty}^{x}\left(\int_{-1}^{\eta_I}\frac{\partial\Phi_L}{\partial x}\,\mathrm{d}z+\lambda_1^2\frac{\partial\eta_I}{\partial v}\right)\mathrm{d}x'.\end{aligned} \tag{3.20b}$$

The key to deriving (3.19) is to note that $\partial\Phi_U/\partial x$, $\partial\Phi_L/\partial x$, $-\lambda_1\mathrm{d}\eta_I/\mathrm{d}x$, and $\lambda_1\left[\rho\partial\Phi_U/\partial x-\partial\Phi_L/\partial x\right]_{z=\eta_I}$ included in (3.13) for $n=3$ are equal to the inhomogeneous terms of (3.4) for $n=2$, (3.5) for $n=2$, (3.7) (or (3.8)) for $n=1$, and (3.9) for $n=1$, respectively, and replace them with the corresponding left-hand-side terms, $\nabla_2^2\hat{\phi}^{(2)}_{UC}$, $\nabla_2^2\hat{\phi}^{(2)}_{LC}$, $\mathrm{L_U}[\hat{\phi}^{(1)}_{UC},\hat{\eta}^{(1)}_C]$ (or $\mathrm{L_L}[\hat{\phi}^{(1)}_{LC},\hat{\eta}^{(1)}_C]$), and $\mathrm{L_I}[\hat{\phi}^{(1)}_{UC},\hat{\phi}^{(1)}_{LC},\hat{\eta}^{(1)}_C]$. We then integrate the result by parts to obtain (3.19). The $[\hat{\phi}^{(1)}_{UC}]_{x\to-\infty}$, $[\hat{\phi}^{(1)}_{LC}]_{x\to-\infty}$, $[\hat{u}^{(2)}_{UC}]_{x\to-\infty}$, and $[\hat{u}^{(2)}_{LC}]_{x\to-\infty}$ appearing on the right-hand side of (3.19) are related to the corresponding values as $x\to\infty$ by

$$\left[\hat{\phi}^{(1)}_{UC}\right]_{x\to-\infty}=\left[\hat{\phi}^{(1)}_{UC}\right]_{x\to\infty}-\frac{\lambda_1}{D}\frac{\mathrm{d}}{\mathrm{d}v}\left(vM+\frac{2T_U}{\rho v}\right), \tag{3.21a}$$

$$\left[\hat{\phi}^{(1)}_{LC}\right]_{x\to-\infty}=\left[\hat{\phi}^{(1)}_{LC}\right]_{x\to\infty}+\lambda_1\frac{\mathrm{d}}{\mathrm{d}v}\left(vM-\frac{2T_L}{v}\right), \tag{3.21b}$$

$$\left[\hat{u}^{(2)}_{UC}\right]_{x\to-\infty}=\left[\hat{u}^{(2)}_{UC}\right]_{x\to\infty}-vM-\lambda_1^2\frac{\mathrm{d}M}{\mathrm{d}v}, \tag{3.21c}$$

https://doi.org/10.1017/S0022112008002802 Published online by Cambridge University Press

$$\left[\hat{u}_{LC}^{(2)}\right]_{x\to-\infty} = \left[\hat{u}_{LC}^{(2)}\right]_{x\to\infty} - vM - \lambda_1^2\frac{\mathrm{d}M}{\mathrm{d}v}, \tag{3.21d}$$

where M, T_U, and T_L are defined by (2.28b–d). We can easily estimate that λ_2 in (3.19) will have non-zero real part in view of (3.21). Thus, the core solution is obtained up to the orders that can determine the stability of the solitary wave both for $\mathrm{d}E/\mathrm{d}v<0$ and $\mathrm{d}E/\mathrm{d}v>0$. The $[\hat{\phi}_{UC}^{(1)}]_{x\to\infty}$, $[\hat{\phi}_{LC}^{(1)}]_{x\to\infty}$, $[\hat{u}_{UC}^{(2)}]_{x\to\infty}$, and $[\hat{u}_{LC}^{(2)}]_{x\to\infty}$, which are necessary for determining the specific value of λ_2 in (3.19), are given after matching the core solution with the far-field solution. The far-field solution is given in Appendix B and the matching is accomplished in Appendix C. The results for $[\hat{\phi}_{UC}^{(1)}]_{x\to\infty}$, $[\hat{\phi}_{LC}^{(1)}]_{x\to\infty}$, $[\hat{u}_{UC}^{(2)}]_{x\to\infty}$, and $[\hat{u}_{LC}^{(2)}]_{x\to\infty}$ can be found in (C6a–d) and (C7a–d).

Substituting (3.21) with (C6a–d) or (C7a–d) into (3.19), we have

$$\lambda_2 = \lambda_1\left\{-\frac{Q}{|\lambda_1|} + \frac{\rho v}{(\rho+D)\mathrm{d}E/\mathrm{d}v}\left[\frac{\mathrm{d}}{\mathrm{d}v}\left(\frac{T_U/\rho+T_L}{v}\right)\right]^2\right\} \tag{3.22a}$$

for $\mathrm{d}E/\mathrm{d}v<0$, and

$$\lambda_2 = \begin{cases} \pm Q + \dfrac{\rho v\lambda_1}{(\rho+D)\mathrm{d}E/\mathrm{d}v}\left[\dfrac{\mathrm{d}}{\mathrm{d}v}\left(\dfrac{T_U/\rho+T_L}{v}\right)\right]^2 & \text{if } Q<0, \\ \text{no solution} & \text{if } Q>0, \end{cases} \tag{3.22b}$$

for $\mathrm{d}E/\mathrm{d}v>0$, where

$$Q = \frac{v^2E}{2(\mathrm{d}E/\mathrm{d}v)^2}\left(\frac{\mathrm{d}M}{\mathrm{d}v} - \frac{M}{E}\frac{\mathrm{d}E}{\mathrm{d}v}\right)\frac{\mathrm{d}\Omega}{\mathrm{d}v}. \tag{3.23}$$

Thus, the eigenvalue λ is explicitly obtained up to the second order in ε by (3.2) with (3.18) and (3.22). The corresponding eigenfunctions are (3.3) with (3.1), (3.14), and (3.17) for the core solution, and (B2) with (B17), (B21), and (C6e–h) or (C7e–h) for the far-field solution. It should be noted that, when $\rho=0$ and $\mathrm{d}E/\mathrm{d}v>0$, Q given by (3.23) in the present study reduces to Q defined by (3.40) of Kataoka & Tsutahara (2004a), where surface solitary waves were treated for $\mathrm{d}E/\mathrm{d}v>0$. In the same way, the eigenvalues and eigenfunctions in the present study correspond with those of Kataoka & Tsutahara (2004a) when $\rho=0$ and $\mathrm{d}E/\mathrm{d}v>0$ (specifically in their paper the eigenvalues are (3.2) with (3.11) and (3.39), the eigenfunctions for the core solution are (3.3) with (3.1) and (3.9), and those for the far-field solution are (3.18) with (3.22), (3.26), (3.30), and (3.37 c–e) or (3.38 c–e) of Kataoka & Tsutahara (2004a).

From (3.18) and (3.22b), there exists a solution for which λ has a positive real part if $\mathrm{d}E/\mathrm{d}v<0$ or $Q<0$. Now we can say that

$$\frac{\mathrm{d}E}{\mathrm{d}v}<0 \quad \text{or} \quad Q<0 \tag{3.24}$$

is a sufficient condition for the transverse instability of interfacial solitary waves, where E and Q are defined by (2.26) and (3.23), respectively.

It should be noted that the above stability analysis is based on the full Euler equations. In the limit of small amplitude, our results agree with those based on the Kadomtsev–Petviashivili (KP) equation. See Appendix D for details.

A remark should be given for the case when a solitary wave steepens to have vertical tangent and overhangs (Meiron & Saffman 1983; Amick & Turner 1986; Pullin & Grimshaw 1988; Sha & Vanden-Broeck 1993; Laget & Dias 1997; Rusås & Grue 2002). In this case, the interfacial displacement η_I of the solitary wave has an infinite

https://doi.org/10.1017/S0022112008002802 Published online by Cambridge University Press

slope ($|\mathrm{d}\eta_I/\mathrm{d}x| = \infty$). One may consider that the appearance of a singular term for the component function $\hat{\eta}_C^{(0)} = \mathrm{d}\eta_I/\mathrm{d}x$ (see (3.1)) may invalidate the above asymptotic analysis. However, the basic equations (3.4)–(3.10) can be reduced to a form in which $\hat{\eta}_C^{(n)}$ appear solely as $\hat{\eta}_C^{(n)}\cos\theta$, where $\theta = \arctan(\mathrm{d}\eta_I/\mathrm{d}x)$. Since $\hat{\eta}_C^{(0)}\cos\theta = \sin\theta$ is finite and smooth at vertical tangent $\theta = \pm\pi/2$, the singularity essentially disappears in the basic equations (3.4)–(3.10) and the above analysis is valid for the overhanging solitary waves. See Kataoka (2006, Sections 2 and 3.1.1) for more details on this point.

4. Derivation of a general statement

We show that the sufficient condition (3.24) for the transverse instability leads to the following general statement on the stability of interfacial solitary waves.

PROPOSITION. *Suppose that the interfacial solitary wave solutions do not bifurcate, and trace the branch of solitary wave solutions for fixed ρ and D from small amplitude. Suppose also that v and M never become stationary at the first stationary value of E. Then, the solitary waves become transversely unstable before an exchange of longitudinal stability occurs.*

Proof. If the solitary wave solutions do not bifurcate, and v never becomes stationary at the first stationary value of E, an exchange of longitudinal stability occurs at the first stationary value of E around which (2.27) holds (Kataoka 2006). From (2.27) and the fact that the first exchange of longitudinal stability generates a growing disturbance mode (because small-amplitude solitary waves are stable (Jeffery & Kakutani 1970; Benjamin 1972)), an inequality $(\mathrm{d}E/\mathrm{d}v)(\mathrm{d}M/\mathrm{d}v)(\mathrm{d}\Omega/\mathrm{d}v) < 0$, i.e.

$$\frac{\mathrm{d}E}{\mathrm{d}v} < 0 \quad \text{or} \quad \frac{\mathrm{d}M}{\mathrm{d}v}\frac{\mathrm{d}\Omega}{\mathrm{d}v} < 0 \tag{4.1}$$

holds if one approaches the first point of $\mathrm{d}E/\mathrm{d}v = 0$ from the small-amplitude side. Moreover, from the hypothesis that M never becomes stationary at the first stationary value of E, an inequality

$$\left|\frac{M}{E}\frac{\mathrm{d}E}{\mathrm{d}v}\right| < \left|\frac{\mathrm{d}M}{\mathrm{d}v}\right| \tag{4.2}$$

holds if one approaches the first point of $\mathrm{d}E/\mathrm{d}v = 0$. A combination of (4.1) and (4.2) satisfies the sufficient condition (3.24) for the transverse instability. □

It should be noted that the hypothesis introduced in the proposition that the solitary wave solutions do not bifurcate means that a new solution branch never appears from the regular solution branch for given ρ and D. This hypothesis together with the other hypothesis that v and M never become stationary at the first stationary value of E, will hold in general because numerical results in the previous studies have provided no evidence of violating these hypotheses (Funakoshi & Oikawa 1986; Pullin & Grimshaw 1988; Kataoka 2006). Examples of the solitary wave solution branches are shown in figure 2(*a–c*), while some specific values of v, E, and M are shown in table 1 (wave amplitude h in table 1 is defined by (5.1) below).

5. Stability of specific solitary waves

Let us apply the criterion (3.24) to specific solitary wave solutions. For a clear intuitive picture of the wave form, we here define the wave amplitude of the solitary

https://doi.org/10.1017/S0022112008002802 Published online by Cambridge University Press

$(D, \rho) = (1,\ 0.0006)$				$(D, \rho) = (3,\ 0.03)$				$(D, \rho) = (10,\ 0.1)$			
h	v	E	M	h	v	E	M	h	v	E	M
0.76	1.29180	1.0380	2.0795	0.98	1.3267	1.6463	2.5740	1.90	1.5259	7.2230	5.4241
0.77	1.29373	1.0478	2.0809	1.00	1.3307	1.6762	2.5778	1.92	1.5300	7.3308	5.4339
0.78	1.29552	1.0566	**2.0812**	1.02	1.3345	1.7032	**2.5783**	1.94	1.5339	7.4332	**5.4387**
0.79	1.29716	1.0642	2.0805	1.04	1.3380	1.7268	2.5751	1.96	1.5377	7.5281	5.4374
0.80	1.29864	1.0706	2.0786	1.06	1.3412	1.7461	2.5676	1.98	1.5412	7.6123	5.4278
0.81	1.29993	1.0757	2.0755	1.08	1.3440	1.7598	2.5546	1.99	1.5428	7.6490	5.4188
0.82	1.30101	1.0793	2.0711	1.09	1.3452	1.7640	2.5456	2.00	1.5444	7.6806	5.4062
0.83	1.30187	1.0813	2.0654	1.10	1.3463	**1.7661**	2.5345	2.01	1.5458	7.7055	5.3888
0.84	1.30248	**1.0815**	2.0583	1.11	1.3471	1.7655	2.5209	2.02	1.5471	7.7212	5.3649
0.85	1.30283	1.0800	2.0497	1.12	1.3477	1.7615	2.5042	2.03	1.5481	**7.7226**	5.3310
0.86	**1.30289**	1.0767	2.0397	1.13	**1.3480**	1.7531	2.4834	2.04	**1.5485**	7.6973	5.2787
0.87	1.30266	1.0716	2.0284	1.14	1.3475	1.7383	2.4568	2.05	1.5471	7.5762	5.1603

TABLE 1. Wave speeds v, total wave energies E, and masses M of interfacial solitary waves as functions of wave amplitude h. The cases $(D, \rho) = (1, 0.0006)$, (3,0.03), and (10,0.1) are shown. The bold-face letters indicate the first extreme values when a solution branch is traced from small amplitude ($h \ll 1$).

wave by the dimensionless maximum interfacial displacement

$$h \equiv \max |\eta_I| \,. \tag{5.1}$$

Depending on the situation, we use either v or h as one of the parameters of the solitary wave. The interfacial solitary waves are characterized by either (ρ, D, v) or (ρ, D, h). In § 2 the existence of the solitary wave solution was discussed in terms of the former set (ρ, D, v) (see the paragraph including (2.20)). Here we make the same discussion in terms of (ρ, D, h). The condition for the existence of the solitary wave solution is

$$0 < h < H, \tag{5.2}$$

where H is a limiting wave amplitude of the solitary wave that takes the following values:

(i) When ρ is larger than some critical value, or $\rho > \rho_{\rm cr}(D)$, where $\rho_{\rm cr}(D)$ is an increasing function of D specifically given by (2.22), H is equal to the amplitude of internal bores:

$$H = \frac{|D - \sqrt{\rho}|}{1 + \sqrt{\rho}} \quad \text{for} \quad \rho > \rho_{\rm cr}(D) \tag{5.3}$$

(Funakoshi & Oikawa 1986; Laget & Dias 1997; Dias & Vanden-Broeck 2003).

(ii) When ρ is smaller than the above critical value, or $\rho < \rho_{\rm cr}(D)$, H is smaller than the amplitude of internal bores:

$$H < \frac{|D - \sqrt{\rho}|}{1 + \sqrt{\rho}} \quad \text{for} \quad \rho < \rho_{\rm cr}(D), \tag{5.4}$$

and a precise limiting amplitude H in this case is not found due to the computational difficulty of specifying it.

The solitary wave solutions, whose existence is discussed in terms of (ρ, D, v) in § 2 and in terms of (ρ, D, h) in the previous paragraph, are numerically calculated using the method described in Turner & Vanden-Broeck (1988). For $\rho < D^2$ (which can be either $\rho < \rho_{\rm cr}(D)$ or $\rho > \rho_{\rm cr}(D)$) the solitary waves are of elevation type, and for

https://doi.org/10.1017/S0022112008002802 Published online by Cambridge University Press

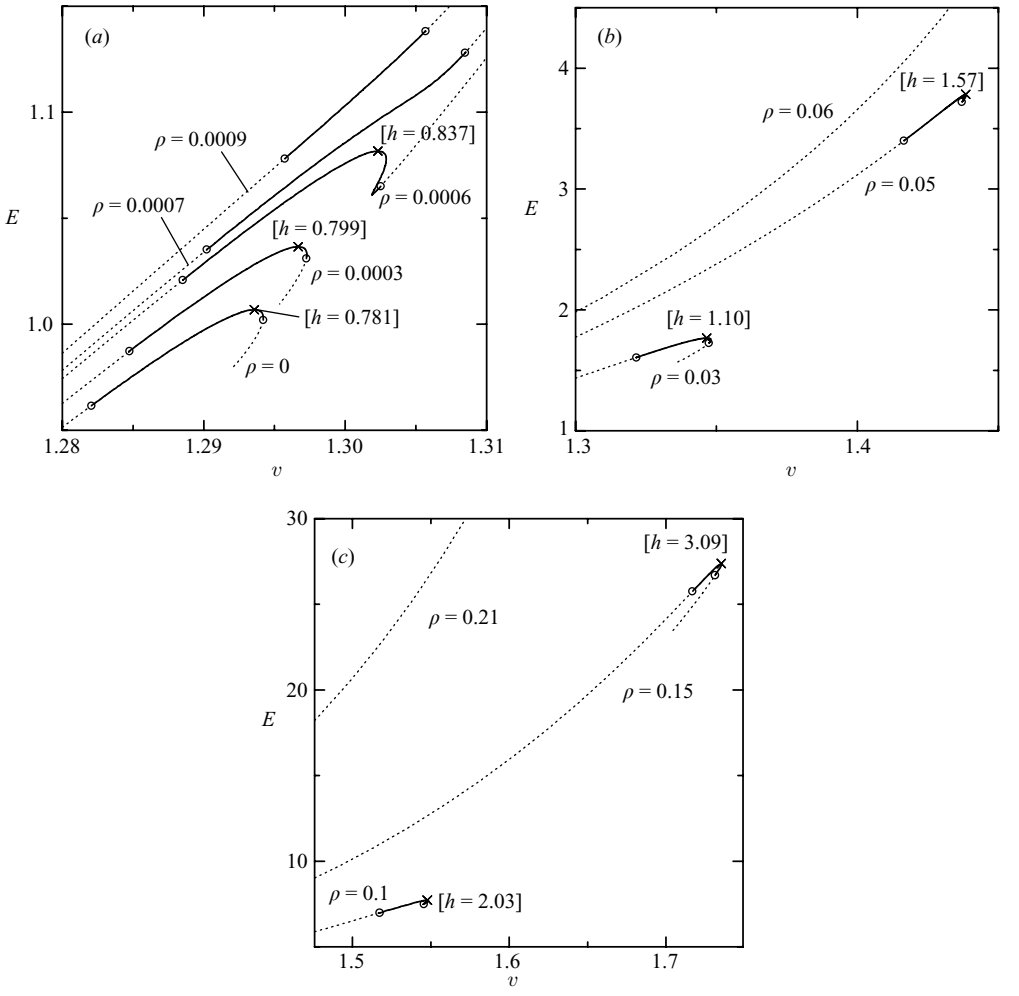


FIGURE 2. Total wave energy E versus wave speed v of interfacial solitary waves: (*a*) $D=1$; (*b*) $D=3$; (*c*) $D=10$. On the solid lines whose end points are denoted by the circles, the solitary waves satisfy the sufficient condition (3.24) for the transverse instability. The positions of the circles are determined by $Q=0$, and $Q<0$ for the solid lines. For $\rho \geqslant 0.001$ ($D=1$), $\rho \geqslant 0.06$ ($D=3$), and $\rho \geqslant 0.21$ ($D=10$), there are no solitary waves that satisfy the condition (3.24) for the transverse instability. The crosses represent the points of $\mathrm{d}E/\mathrm{d}v=0$ at which an exchange of longitudinal stability first occurs when a solution branch is traced from small amplitude $(v, E)=(c, 0)$ (see (2.20)). The corresponding critical amplitudes h at the crosses are shown in the square brackets. The upper limiting values $v=V$ (see (2.23)) of the wave speed for $\rho > \rho_{\mathrm{cr}}(D)$ are, for instance, $V=1.38$, 1.38, 1.37, 1.56, and 2.02 when $(\rho, D)=(0.0006, 1)$, (0.0007,1), (0.001,1), (0.06,3), and (0.21,10), respectively.

$\rho > D^2$ (which can only be $\rho > \rho_{\mathrm{cr}}(D)$) they are of depression type (Amick & Turner 1986; Funakoshi & Oikawa 1986). The former is treated in § 5.1 and the latter in § 5.2.

5.1. *Solitary waves of elevation* ($\rho < D^2$)

Figure 2 shows the total wave energy E of solitary waves versus wave speed v for various values of $\rho(<D^2)$, when $D=1$, 3, and 10. The upper limiting values $v=V$ of the wave speed for $\rho > \rho_{\mathrm{cr}}(D)$ defined by (2.23) are given in the figure caption. In figure 2, the crosses denote the points of $\mathrm{d}E/\mathrm{d}v=0$ at which an exchange of longitudinal stability first occurs when a solution branch is traced from small

https://doi.org/10.1017/S0022112008002802 Published online by Cambridge University Press

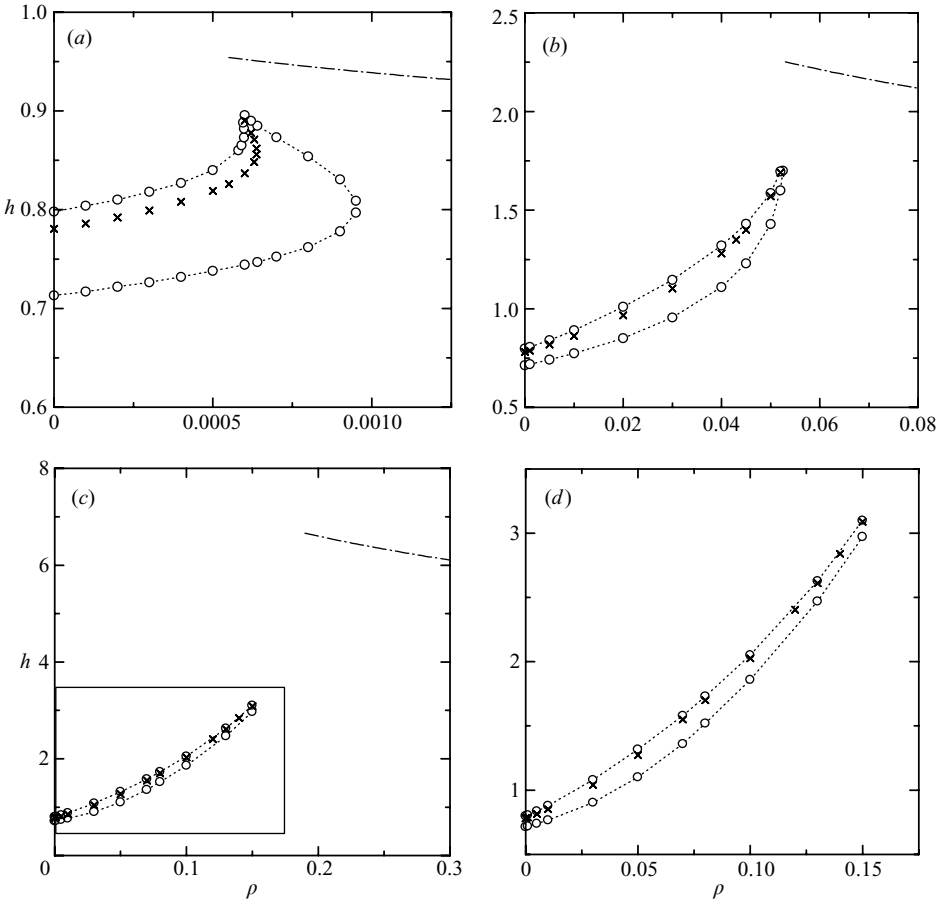


FIGURE 3. Critical amplitudes h at which interfacial solitary waves first begin or cease to satisfy the sufficient condition (3.24) for the transverse instability (denoted by the circles) and those h at which an exchange of longitudinal stability first occurs (denoted by the crosses) when a solution branch is traced from small amplitude ($h \ll 1$). (*a*) $D = 1$; (*b*) $D = 3$; (*c*) $D = 10$; (*d*) blow up of the rectangular region in (*c*). Positions of the circles are all determined by $Q = 0$. The solitary waves satisfy the sufficient condition (3.24) for the transverse instability in a parameter region enclosed by the dotted lines which connect the circles and the h-axis. The crosses are all located in this region. The dash-dot lines show the limiting wave amplitude $h = H$ (see (5.3)) for $\rho > \rho_{\rm cr}(D)$.

amplitude. The solitary wave solutions satisfy the sufficient condition (3.24) for the transverse instability on the solid lines whose end points are denoted by the circles. From figure 2, we see that any crosses are located on the solid lines. When a solution branch is traced from small amplitude, therefore, the solitary waves become transversely unstable before an exchange of longitudinal stability occurs, as stated in the proposition.

Figure 3 plots various critical amplitudes on a (ρ, h)-plane for $D = 1$, 3, and 10 (figure 3*d* is a blow up of the rectangular region in figure 3*c*). The crosses are the recognized critical amplitudes of $\mathrm{d}E/\mathrm{d}v = 0$ at which an exchange of longitudinal stability first occurs, and the open circles are those at which the solitary waves of elevation first begin or cease to satisfy the sufficient condition (3.24) for the transverse instability when a solution branch is traced from small amplitude ($h \ll 1$). The dash-dot lines represent the limiting wave amplitude $h = H$ for $\rho > \rho_{\rm cr}(D)$ defined by (5.3).

https://doi.org/10.1017/S0022112008002802 Published online by Cambridge University Press

$D=1$			$D=3$			$D=10$		
ρ	h_T	(h_L)	ρ	h_T	(h_L)	ρ	h_T	(h_L)
0.0001	0.717	(0.786)	0.0001	0.714	(0.781)	0.0001	0.714	(0.781)
0.0002	0.722	(0.792)	0.001	0.719	(0.788)	0.001	0.718	(0.787)
0.0003	0.726	(0.799)	0.005	0.742	(0.819)	0.005	0.739	(0.814)
0.0004	0.732	(0.808)	0.01	0.774	(0.862)	0.01	0.766	(0.851)
0.0005	0.738	(0.819)	0.02	0.851	(0.967)	0.02	0.829	(0.936)
0.0006	0.744	(0.837)	0.03	0.956	(1.10)	0.05	1.10	(1.27)
0.0007	0.752	(–)	0.04	1.11	(1.28)	0.1	1.86	(2.03)
0.0009	0.778	(–)	0.05	1.43	(1.57)	0.15	2.97	(3.09)
0.001	–	(–)	0.06	–	(–)	0.21	–	(–)

TABLE 2. Critical amplitudes at which the solitary waves of elevation first begin to satisfy the sufficient condition (3.24) for the transverse instability (denoted by h_T) and those at which an exchange of longitudinal stability first occurs (denoted by h_L in the parentheses) when a solution branch is traced from small amplitude. The cases $D=1$, 3, 10 are presented. The – indicates that there is no corresponding critical amplitude.

Multiple solitary wave solutions may exist for given h of course. In such case, the stability given by figure 3 applies to the first solitary wave that reaches a given h when a solution branch is traced from small amplitude. In these figures the solitary waves satisfy the sufficient condition (3.24) for the transverse instability in the parameter region enclosed by the dotted lines (which connect the circles) and the h-axis. We see that the crosses are all located inside this region of transverse instability, indicating that the critical amplitude for an exchange of longitudinal stability is always larger than that of the transverse instability for given ρ and D. In table 2, these two critical amplitudes are given for various values of ρ, and $D=1$, 3, and 10.

5.2. *Solitary waves of depression* ($\rho > D^2$)

For all the solitary waves of depression investigated by us, $\mathrm{d}E/\mathrm{d}v$ is always positive, indicating that no exchange of longitudinal stability occurs, and the sufficient condition (3.24) for the transverse instability is never satisfied.

6. Physical interpretation

Let us discuss the physical mechanism of the transverse instability by considering the meaning of the analytical solution obtained in § 3. The solution was obtained from the linearized equations (2.29)–(2.36) for disturbances, so that quantities involving the square of disturbances are neglected here. On the basis of the linearized equations, we sought an asymptotic solution for small transverse wavenumbers ε of disturbances. The corresponding core solution up to $O(\varepsilon^2)$ is given by (3.3) with (3.1), (3.14), and (3.17), and it represents distortion in the phase shift and the wave speed of the solitary wave, plus generation of a residual to it:

$$\begin{pmatrix} \Phi_U(x,z;v)+\hat{\phi}_{UC}\exp(\lambda t+\mathrm{i}\varepsilon y) \\ \Phi_L(x,z;v)+\hat{\phi}_{LC}\exp(\lambda t+\mathrm{i}\varepsilon y) \\ \eta_I(x;v) \quad + \quad \hat{\eta}_C\exp(\lambda t+\mathrm{i}\varepsilon y) \end{pmatrix} = \begin{pmatrix} \Phi_U(x-\delta x,z;v+\delta v) \\ \Phi_L(x-\delta x,z;v+\delta v) \\ \eta_I(x-\delta x;v+\delta v) \end{pmatrix} - \varepsilon^2\delta x \begin{pmatrix} \bar{\phi}^{(2)}_{UC} \\ \bar{\phi}^{(2)}_{LC} \\ \bar{\eta}^{(2)}_{C} \end{pmatrix} + O(\varepsilon^3), \tag{6.1}$$

https://doi.org/10.1017/S0022112008002802 Published online by Cambridge University Press

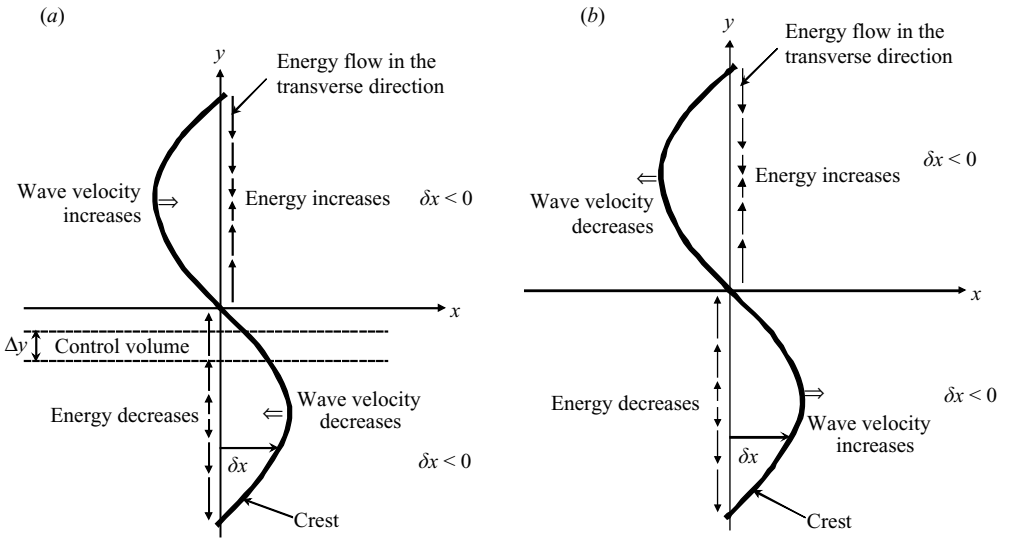


FIGURE 4. The crest of a distorted solitary wave and its motion induced by the energy flow in the transverse direction associated with distortion in the phase shift of the solitary wave. (*a*) $\mathrm{d}E/\mathrm{d}v > 0$ (oscillatory motion); (*b*) $\mathrm{d}E/\mathrm{d}v < 0$ (self-focusing-type instability). The region enclosed by the two dashed lines in (*a*) represents an example of a control volume, and δx represents the phase shift.

where the second term on the right-hand side represents the residual, and

$$\delta x = -\exp(\lambda t + \mathrm{i}\varepsilon y), \quad \delta v = \frac{\partial(\delta x)}{\partial t} \tag{6.2}$$

are the phase shift and a perturbed wave speed of the distorted solitary wave, respectively. A schematic of δx is shown in figure 4 as a function of y, which describes the crest (peak) of the distorted solitary wave at some instantaneous time t.

Let us physically interpret (3.13), which is a time-evolution equation for δ_x. Taking a control volume pinched by two control surfaces $y = \text{constant}$ and $y = \text{constant} + \Delta y$ (see the dashed lines in figure 4*a*), and multiplying (3.13) for $n = 2$ by $\varepsilon^2 v \delta x \Delta y$, we obtain the following leading-order evolution equation:

$$\frac{\partial E(v+\delta v_1)}{\partial t}\Delta y = -\frac{\partial}{\partial y}\int_{-\infty}^{\infty}\left\{\int_{\eta_I}^{D}\left[\frac{\rho}{2}\left(\left(\frac{\partial \Phi_U}{\partial x}\right)^2+\left(\frac{\partial \Phi_U}{\partial z}\right)^2\right)+p\right]\frac{\partial \Phi_U(x-\delta x, z; v)}{\partial y}\,\mathrm{d}z + \int_{-1}^{\eta_I}\left[\frac{1}{2}\left(\left(\frac{\partial \Phi_L}{\partial x}\right)^2+\left(\frac{\partial \Phi_L}{\partial z}\right)^2\right)+p\right]\frac{\partial \Phi_L(x-\delta x, z; v)}{\partial y}\mathrm{d}z\right\}\mathrm{d}x\,\Delta y, \tag{6.3}$$

where $E(v)$ is the energy of the solitary wave per unit transverse width defined by (2.26), and δv_1 is the perturbed wave speed of $O(\varepsilon)$ (or $\delta v = \delta v_1 + \delta v_2 + \ldots$ with $\delta v_n = O(\varepsilon^n)$). In deriving (6.3), we used the following Bernoulli equations for the solitary wave solution in the upper and lower fluid layers, respectively:

$$\rho v \frac{\partial \Phi_U}{\partial x} = \frac{\rho}{2}\left[\left(\frac{\partial \Phi_U}{\partial x}\right)^2+\left(\frac{\partial \Phi_U}{\partial z}\right)^2\right]+p, \quad v\frac{\partial \Phi_L}{\partial x} = \frac{1}{2}\left[\left(\frac{\partial \Phi_L}{\partial x}\right)^2+\left(\frac{\partial \Phi_L}{\partial z}\right)^2\right]+p, \tag{6.4}$$

https://doi.org/10.1017/S0022112008002802 Published online by Cambridge University Press

where $p(x, z)$ is the difference of the pressure of the solitary wave from its hydrostatic value. The left-hand side of (6.3) represents the rate of change of energy $E(v+\delta v_1)\Delta y$ of the distorted solitary wave in the control volume, while the right-hand side represents the rate of energy flow into the control volume through the two control surfaces. The argument $x-\delta x$ of $\partial\Phi_U/\partial y$ and $\partial\Phi_L/\partial y$ indicates that this energy flow is caused by the distortion in the phase shift δx of the solitary wave. Thus, the leading-order evolution equation describes a motion induced by the energy flow in the transverse direction associated with distortion in the phase shift δx of the solitary wave.

The terms on the right-hand side of (6.3) reduce to $-\varepsilon^2 vE\delta x\Delta y$ (see (3.15)), which has an opposite sign to that of δx. The energy of the solitary wave in the control volume, therefore, increases (the left-hand side of (6.3) becomes positive) when $\delta x<0$ and decreases when $\delta x>0$ (see figure 4). For $\mathrm{d}E/\mathrm{d}v>0$, then, the wave speed δv_1 increases when the crest is behind the original position ($\delta x<0$), and decreases when it is ahead ($\delta x>0$), so that δx is subjected to oscillations (figure 4*a*). The stability in this case is not determined by (6.3) but by the higher-order equation. For $\mathrm{d}E/\mathrm{d}v<0$, on the other hand, the wave speed δv_1 decreases when the crest is behind the original position, and increases when it is ahead, so that $|\delta x|$ increases for sufficiently large times and the instability results (figure 4*b*). The transverse instability of this type is called the self-focusing (Ostrovsky & Shrira 1976; Shrira 1980; Kivshar & Pelinovsky 2000).

Let us consider the physical meaning of the next-order equation. Multiplying (3.13) for $n=3$ by $\varepsilon^3 v\delta x\Delta y$ and using (6.4), we obtain the next-order evolution equation:

$$
\begin{aligned}
&2\frac{\partial E(v+\delta v_2)}{\partial t}\Delta y \\
&\quad=-\frac{\partial\hat{E}_2}{\partial t}\Delta y-\frac{\partial}{\partial y}\int_{-\infty}^{\infty}\left\{\int_{\eta_I}^{D}\left[\frac{\rho}{2}\left(\left(\frac{\partial\Phi_U}{\partial x}\right)^2+\left(\frac{\partial\Phi_U}{\partial z}\right)^2\right)+p\right]\frac{\partial\Phi_U(x,z;v+\delta v_1)}{\partial y}\,\mathrm{d}z\right. \\
&\qquad\left.+\int_{-1}^{\eta_I}\left[\frac{1}{2}\left(\left(\frac{\partial\Phi_L}{\partial x}\right)^2+\left(\frac{\partial\Phi_L}{\partial z}\right)^2\right)+p\right]\frac{\partial\Phi_L(x,z;v+\delta v_1)}{\partial y}\mathrm{d}z\right\}\mathrm{d}x\Delta y, \qquad (6.5)
\end{aligned}
$$

where δv_2 is the perturbed wave speed of $O(\varepsilon^2)$, and

$$
\begin{aligned}
\hat{E}_2=-\varepsilon^2\delta x\Bigg\{&\int_{-\infty}^{\infty}\Bigg[-\frac{\rho}{2}\left(\left(\frac{\partial\Phi_U}{\partial x}\right)^2+\left(\frac{\partial\Phi_U}{\partial z}\right)^2\right) \\
&+\frac{1}{2}\left(\left(\frac{\partial\Phi_L}{\partial x}\right)^2+\left(\frac{\partial\Phi_L}{\partial z}\right)^2\right)+(1-\rho)\eta_I\Bigg]_{z=\eta_I}\bar{\eta}_C^{(2)}\,\mathrm{d}x \\
&+\rho\int_{-\infty}^{\infty}\int_{\eta_I}^{D}\left(\frac{\partial\Phi_U}{\partial x}\frac{\partial\bar{\phi}_{UC}^{(2)}}{\partial x}+\frac{\partial\Phi_U}{\partial z}\frac{\partial\bar{\phi}_{UC}^{(2)}}{\partial z}\right)\mathrm{d}x\,\mathrm{d}z \\
&+\int_{-\infty}^{\infty}\int_{-1}^{\eta_I}\left(\frac{\partial\Phi_L}{\partial x}\frac{\partial\bar{\phi}_{LC}^{(2)}}{\partial x}+\frac{\partial\Phi_L}{\partial z}\frac{\partial\bar{\phi}_{LC}^{(2)}}{\partial z}\right)\mathrm{d}x\,\mathrm{d}z\Bigg\} \qquad (6.6)
\end{aligned}
$$

is the energy due to the product of the solitary wave and the residual $-\varepsilon^2\delta x(\bar{\phi}_{UC}^{(2)},\bar{\phi}_{LC}^{(2)},\bar{\eta}_C^{(2)})$ per unit transverse width. The left-hand side of (6.5) represents the next-order rate of change of energy of the distorted solitary wave in the control volume. The first term on the right-hand side of (6.5) represents the rate of transfer of energy to the residual in the control volume, while the remaining terms are the next-order rate of energy flow into the control volume through the two control surfaces. The parameter $v+\delta v_1$ of $\partial\Phi_U/\partial y$ and $\partial\Phi_L/\partial y$ indicates that this energy flow is caused by distortion in the wave speed δv_1 of the solitary wave. Thus, the next-order

https://doi.org/10.1017/S0022112008002802 Published online by Cambridge University Press

evolution equation describes a motion induced by the two effects: transfer of energy to the residual in the control volume and the energy flow in the transverse direction due to distortion in the wave speed δv_1 of the solitary wave.

For $\mathrm{d}E/\mathrm{d}v > 0$, the sum of the above two effects, given by the right-hand side of (6.5) reduces to a quantity proportional to δx and one proportional to δv_1 as

$$2\frac{\partial E(v+\delta v_2)}{\partial t}\Delta y = -\frac{2\varepsilon^3\rho v^2 E\Delta y}{(\rho+D)\mathrm{d}E/\mathrm{d}v}\left[\frac{\mathrm{d}}{\mathrm{d}v}\left(\frac{T_U/\rho+T_L}{v}\right)\right]^2\delta x + 2\varepsilon^2\frac{\mathrm{d}E}{\mathrm{d}v}\Delta y \times \begin{cases}(-Q\delta v_1) & \text{when } \left[\bar{\eta}_C^{(2)}\right]_{x\to\infty}=0,\\ Q\delta v_1 & \text{when } \left[\bar{\eta}_C^{(2)}\right]_{x\to-\infty}=0,\end{cases} \tag{6.7}$$

which can be obtained by substituting (3.21) and (C6*a–d*) (when $[\bar{\eta}_C^{(2)}]_{x\to\infty}=0$) or (C7*a–d*) (when $[\bar{\eta}_C^{(2)}]_{x\to-\infty}=0$) into (3.19) multiplied by $\varepsilon^3 v\delta x\Delta y$. The first term proportional to δx on the right-hand side of (6.7) has an opposite sign to δx and only plays the role of modifying the frequency of oscillation when $\mathrm{d}E/\mathrm{d}v > 0$. The second term proportional to δv_1 changes sign depending on whether the residual is accompanied by linear waves propagating ahead of the solitary wave or behind the solitary wave (the propagating linear waves are expressed by the terms including $\exp(k_1 X_1)$ and $\exp(\bar{k}_1 X_1)$ of (B17)). Since the wave speed of a linear wave is smaller than that of the solitary wave, for sufficiently large times there are no linear waves propagating ahead of the solitary wave, or $[\bar{\eta}_C^{(2)}]_{x\to\infty}=0$ (the first case of (6.7)). Thus, from the contribution of the second term on the right-hand side of (6.7), for $Q<0$, the second-order wave energy and speed δv_2 increase (the left-hand side of (6.7) becomes positive) when the crest is moving forward ($\delta v_1 > 0$), and decrease when it is moving backward ($\delta v_1 < 0$), which leads to amplification of the oscillations (see figure 5). This is a new type of instability first found for surface solitary waves (Kataoka & Tsutahara 2004*a*) and discovered for interfacial solitary waves in the present study.

7. Concluding remarks

We have examined the linear stability of finite-amplitude interfacial solitary waves in a two-layer fluid of finite depth on the basis of the Euler equations. An asymptotic analysis is performed, which provides an explicit criterion of instability in the case of long-wavelength transverse disturbances. This result leads to the general statement that, when the branch of the solitary wave solution is traced from small amplitude, the solution becomes transversely unstable before an exchange of longitudinal stability occurs. We then applied the criterion of instability to specific solitary wave solutions, and the results are consistent with the above general statement. Physical interpretation of the analytical solution was also given.

It should be noted that the stability analysis of the present study is based on the full Euler equations. In the limit of small amplitude, our results agree with those based on the KP equation (see Appendix D).

We conclude with two remarks. First, the analysis given in this paper is for the case of finite-depth fluid, because we used the condition that the tail of the solitary wave decays exponentially. When either the upper or the lower fluid is infinitely deep, the tail of the solitary wave decays algebraically (Benjamin 1967; Davis & Acrivos 1967; Pullin & Grimshaw 1988), and an analysis that takes into account the slow decay must be used for the case of infinite depth. Second, the present analysis is limited to the stability to long-wavelength transverse disturbances ($\varepsilon \ll 1$). To study the

https://doi.org/10.1017/S0022112008002802 Published online by Cambridge University Press

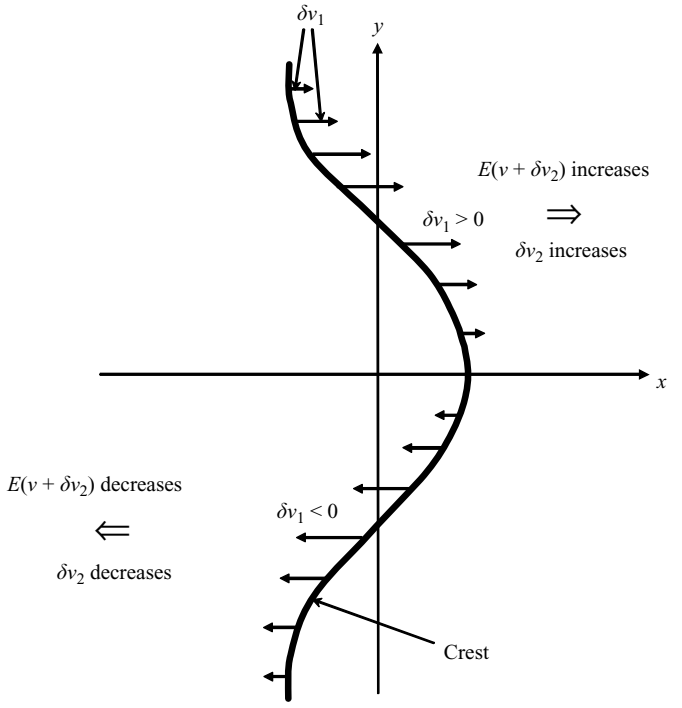


FIGURE 5. The crest of a distorted solitary wave and the mechanism leading to amplification of the oscillations, when $\mathrm{d}E/\mathrm{d}v > 0$ and $Q < 0$. δv_1 and δv_2 are the first- and second-order perturbed wave speeds of the solitary wave, respectively. $E(v+\delta v_2)$ represents the energy of the solitary wave with a second-order variation.

stability to disturbances of finite transverse wavelength ($\varepsilon = O(1)$), we must resort to a numerical means. The present author is now making such a numerical investigation for surface solitary waves ($\rho = 0$), and the results will be reported elsewhere.

The author thanks the referees for their valuable comments and suggestions, which have led to improvement of the paper.

Appendix A. Derivation of (3.16)

Equation (3.16) is obtained if the integrand on its left-hand side, i.e.,

$$\frac{\rho}{2}\int_{\eta_I}^{D}\left[\left(\frac{\partial \Phi_U}{\partial x}\right)^2-\left(\frac{\partial \Phi_U}{\partial z}\right)^2\right]\mathrm{d}z+\frac{1}{2}\int_{-1}^{\eta_I}\left[\left(\frac{\partial \Phi_L}{\partial x}\right)^2-\left(\frac{\partial \Phi_L}{\partial z}\right)^2\right]\mathrm{d}z-\frac{1-\rho}{2}\eta_I^2 \tag{A 1}$$

vanishes. Differentiating (A1) with respect to x and using integration by parts with the aid of (2.11)–(2.15) and (2.17), we have

$$\frac{\mathrm{d(A1)}}{\mathrm{d}x}=\left[\left\{-\frac{\rho}{2}\left(\left(\frac{\partial \Phi_U}{\partial x}\right)^2-\left(\frac{\partial \Phi_U}{\partial z}\right)^2\right)+\frac{1}{2}\left(\left(\frac{\partial \Phi_L}{\partial x}\right)^2-\left(\frac{\partial \Phi_L}{\partial z}\right)^2\right)-(1-\rho)\eta_I\right\}\frac{\mathrm{d}\eta_I}{\mathrm{d}x}+\rho\frac{\partial \Phi_U}{\partial x}\frac{\partial \Phi_U}{\partial z}-\frac{\partial \Phi_L}{\partial x}\frac{\partial \Phi_L}{\partial z}\right]_{z=\eta_I}$$

https://doi.org/10.1017/S0022112008002802 Published online by Cambridge University Press

$$= \left[-\rho v \frac{\partial \Phi_U}{\partial x} + \frac{\rho}{2} \left(\left(\frac{\partial \Phi_U}{\partial x} \right)^2 + \left(\frac{\partial \Phi_U}{\partial z} \right)^2 \right) + v \frac{\partial \Phi_L}{\partial x} \right.$$
$$\left. - \frac{1}{2} \left(\left(\frac{\partial \Phi_L}{\partial x} \right)^2 + \left(\frac{\partial \Phi_L}{\partial z} \right)^2 \right) - (1-\rho)\eta_I \right]_{z=\eta_I} \frac{\mathrm{d}\eta_I}{\mathrm{d}x},$$

where (2.11)–(2.13) and (2.17) are used to obtain the first equality, and (2.14) and (2.15) to obtain the last equality. From (2.16), the above far-right side vanishes. The x-derivative of (A1) therefore vanishes, and from (2.18), (A1) itself vanishes.

Appendix B. Far-field solution

The core solution obtained in § 3 has non-zero values as $x \to \pm\infty$, and does not satisfy the decaying boundary conditions (2.36). The reason for this is that the terms including λ and those including $v\mathrm{d}/\mathrm{d}x$ (or $v\partial/\partial x$) are not balanced in (2.32)–(2.34). Since λ will have non-zero real part at $O(\varepsilon)$ or $O(\varepsilon^2)$ (see the statement after (3.21d)), the solution will decay over the distance of $x = O(\varepsilon^{-1})$ or $O(\varepsilon^{-2})$ through the balance of these terms. The balance is achieved by introducing the following reduced coordinates with respect to x:

$$X_1 = \varepsilon x, \quad X_2 = \varepsilon^2 x. \tag{B 1}$$

We then seek a solution of (2.29)–(2.35) with a moderate variation in X_1, X_2, and z ($\partial\hat{h}/\partial X_1 = O(\hat{h})$, $\partial\hat{h}/\partial X_2 = O(\hat{h})$, and $\partial\hat{h}/\partial z = O(\hat{h})$, where $\hat{h}$ represents $(\hat{\phi}_U, \hat{\phi}_L, \hat{\eta})$), in the following power series of ε:

$$\hat{\phi}_{UF} = \varepsilon\hat{\phi}^{(1)}_{UF}(X_1, X_2, z) + \varepsilon^2\hat{\phi}^{(2)}_{UF}(X_1, X_2, z) + \cdots, \tag{B 2a}$$
$$\hat{\phi}_{LF} = \varepsilon\hat{\phi}^{(1)}_{LF}(X_1, X_2, z) + \varepsilon^2\hat{\phi}^{(2)}_{LF}(X_1, X_2, z) + \cdots, \tag{B 2b}$$
$$\hat{\eta}_F = \varepsilon^2\hat{\eta}^{(2)}_F(X_1, X_2) + \varepsilon^3\hat{\eta}^{(3)}_F(X_1, X_2) + \cdots, \tag{B 2c}$$

where the subscript F is attached to indicate the type of solution (far-field solution). The series (B2a–c) start from $O(\varepsilon)$, $O(\varepsilon)$, and $O(\varepsilon^2)$ for $\hat{\phi}_{UF}$, $\hat{\phi}_{LF}$, and $\hat{\eta}_F$, respectively, in accordance with the core solution having non-zero values as $x \to \pm\infty$ from these orders (see (3.21)).

Substituting (B1) and (B2) into (2.29)–(2.35), and collecting the same-order terms in ε, we obtain a series of equations for $(\hat{\phi}^{(n)}_{UF}, \hat{\phi}^{(n)}_{LF}, \hat{\eta}^{(n+1)}_F)$ $(n = 1, 2, \ldots)$:

$$\frac{\partial^2\hat{\phi}^{(n)}_{UF}}{\partial z^2} = I^{(n)} \quad \text{for } 0 < z < D, \tag{B 3}$$

$$\frac{\partial^2\hat{\phi}^{(n)}_{LF}}{\partial z^2} = J^{(n)} \quad \text{for } -1 < z < 0, \tag{B 4}$$

$$\frac{\partial\hat{\phi}^{(n)}_{UF}}{\partial z} = 0 \quad \text{at} \quad z = D, \tag{B 5}$$

$$\frac{\partial\hat{\phi}^{(n)}_{UF}}{\partial z} = K^{(n)}, \quad \frac{\partial\hat{\phi}^{(n)}_{LF}}{\partial z} = K^{(n)} \quad \text{at} \quad z = 0, \tag{B6a,b}$$

$$\left(v\frac{\partial}{\partial X_1} - \lambda_1 \right) \left(\rho\hat{\phi}^{(n)}_{UF} - \hat{\phi}^{(n)}_{LF} \right) + (1-\rho)\hat{\eta}^{(n+1)}_F = L^{(n)} \quad \text{at} \quad z = 0, \tag{B 7}$$

$$\frac{\partial\hat{\phi}^{(n)}_{LF}}{\partial z} = 0 \quad \text{at} \quad z = -1, \tag{B 8}$$

https://doi.org/10.1017/S0022112008002802 Published online by Cambridge University Press

where

$$I^{(n)} = \hat{\phi}_{UF}^{(n-2)} - \frac{\partial^2 \hat{\phi}_{UF}^{(n-2)}}{\partial X_1^2} - 2\frac{\partial^2 \hat{\phi}_{UF}^{(n-3)}}{\partial X_1 \partial X_2} - \frac{\partial^2 \hat{\phi}_{UF}^{(n-4)}}{\partial X_2^2}, \tag{B 9}$$

$$J^{(n)} = \hat{\phi}_{LF}^{(n-2)} - \frac{\partial^2 \hat{\phi}_{LF}^{(n-2)}}{\partial X_1^2} - 2\frac{\partial^2 \hat{\phi}_{LF}^{(n-3)}}{\partial X_1 \partial X_2} - \frac{\partial^2 \hat{\phi}_{LF}^{(n-4)}}{\partial X_2^2}, \tag{B 10}$$

$$K^{(n)} = \left(\lambda_1 - v\frac{\partial}{\partial X_1}\right)\hat{\eta}_F^{(n-1)} + \left(\lambda_2 - v\frac{\partial}{\partial X_2}\right)\hat{\eta}_F^{(n-2)} + \sum_{m=3}^{n-2} \lambda_m \hat{\eta}_F^{(n-m)}, \tag{B 11}$$

$$L^{(n)} = \left(\lambda_2 - v\frac{\partial}{\partial X_2}\right)\left(\rho\hat{\phi}_{UF}^{(n-1)} - \hat{\phi}_{LF}^{(n-1)}\right) + \sum_{m=3}^{n} \lambda_m \left(\rho\hat{\phi}_{UF}^{(n-m+1)} - \hat{\phi}_{LF}^{(n-m+1)}\right). \tag{B 12}$$

Note that $\hat{\phi}_{UF}^{(m)}$ and $\hat{\phi}_{LF}^{(m)}$ for $m \leqslant 0$ and $\hat{\eta}_F^{(m)}$ for $m \leqslant 1$ on the right-hand sides of (B9)–(B12) are zero.

For $n = 1$ and 2, the above set of equations (B3)–(B8) is homogeneous and has a solution independent of z:

$$\hat{\phi}_{UF}^{(1)} = \hat{\phi}_{UF}^{(1)}(X_1, X_2), \quad \hat{\phi}_{LF}^{(1)} = \hat{\phi}_{LF}^{(1)}(X_1, X_2), \tag{B13a,b}$$

$$\hat{\eta}_F^{(2)} = \frac{1}{1-\rho}\left(\lambda_1 - v\frac{\partial}{\partial X_1}\right)\left[\rho\hat{\phi}_{UF}^{(1)} - \hat{\phi}_{LF}^{(1)}\right]_{z=0}, \tag{B13c}$$

and

$$\hat{\phi}_{UF}^{(2)} = \hat{\phi}_{UF}^{(2)}(X_1, X_2), \quad \hat{\phi}_{LF}^{(2)} = \hat{\phi}_{LF}^{(2)}(X_1, X_2), \tag{B14a,b}$$

$$\hat{\eta}_F^{(3)} = \frac{1}{1-\rho}\left(\lambda_1 - v\frac{\partial}{\partial X_1}\right)\left[\rho\hat{\phi}_{UF}^{(2)} - \hat{\phi}_{LF}^{(2)}\right]_{z=0} + \frac{1}{1-\rho}\left(\lambda_2 - v\frac{\partial}{\partial X_2}\right)\left[\rho\hat{\phi}_{UF}^{(1)} - \hat{\phi}_{LF}^{(1)}\right]_{z=0}, \tag{B14c}$$

where the quantities in the square brackets with subscript $z = 0$ are evaluated at $z = 0$.

For $n = 3, 4, \ldots$, the set of equations (B3)–(B8) is inhomogeneous. For this set to have a solution, its inhomogeneous terms $I^{(n)}$, $J^{(n)}$, and $K^{(n)}$ must satisfy the solvability conditions:

$$-\int_0^D I^{(n)} \mathrm{d}z = \int_{-1}^0 J^{(n)} \mathrm{d}z = K^{(n)}. \tag{B 15}$$

For $n = 3$, (B15) become

$$\left[(v^2 - c^2)\frac{\partial^2}{\partial X_1^2} - 2v\lambda_1\frac{\partial}{\partial X_1} + \lambda_1^2 + c^2\right]\left(\rho\hat{\phi}_{UF}^{(1)} - \hat{\phi}_{LF}^{(1)}\right) = 0, \tag{B 16a}$$

$$\left(\frac{\partial^2}{\partial X_1^2} - 1\right)\left(D\hat{\phi}_{UF}^{(1)} + \hat{\phi}_{LF}^{(1)}\right) = 0, \tag{B 16b}$$

where c and λ_1 are given by (2.21) and (3.18), respectively. Equations (B16) together with (B13c) determine the dependence of $(\hat{\phi}_{UF}^{(1)}, \hat{\phi}_{LF}^{(1)}, \hat{\eta}_F^{(2)})$ on X_1 as

$$\hat{\phi}_{UF}^{(1)} = -\frac{q\exp(k_1 X_1) + \bar{q}\exp(\bar{k}_1 X_1)}{D} + r\exp(X_1) + \bar{r}\exp(-X_1), \tag{B 17a}$$

$$\hat{\phi}_{LF}^{(1)} = q\exp(k_1 X_1) + \bar{q}\exp(\bar{k}_1 X_1) + \rho\left[r\exp(X_1) + \bar{r}\exp(-X_1)\right], \tag{B 17b}$$

https://doi.org/10.1017/S0022112008002802 Published online by Cambridge University Press

$$\hat{\eta}_F^{(2)} = \frac{(v\beta + c)q\exp(k_1 X_1) - (v\beta - c)\bar{q}\exp(\bar{k}_1 X_1)}{c(v^2 - c^2)}\lambda_1, \tag{B 17c}$$

where q, $\bar{q}$, r, and $\bar{r}$ are undetermined functions of X_2. The k_1 and $\bar{k}_1$ are the following given constants:

$$k_1 = \frac{v + \beta c}{v^2 - c^2}\lambda_1, \quad \bar{k}_1 = \frac{v - \beta c}{v^2 - c^2}\lambda_1, \tag{B18a,b}$$

where

$$\beta = \begin{cases} \mathrm{i}\sqrt{-\left(1 + \dfrac{v^2 - c^2}{vE}\dfrac{\mathrm{d}E}{\mathrm{d}v}\right)} & \text{for } \dfrac{\mathrm{d}E}{\mathrm{d}v} < -\dfrac{vE}{v^2 - c^2}, \\ \sqrt{1 + \dfrac{v^2 - c^2}{vE}\dfrac{\mathrm{d}E}{\mathrm{d}v}} & \text{for } \dfrac{\mathrm{d}E}{\mathrm{d}v} > -\dfrac{vE}{v^2 - c^2}. \end{cases} \tag{B 19}$$

The coefficients $(v + \beta c)/(v^2 - c^2)$ and $(v - \beta c)/(v^2 - c^2)$ in (B18) have positive real parts when $\mathrm{d}E/\mathrm{d}v < 0$, since $v > c$ (see (2.20)) and $\mathrm{Re}[\beta] < 1$. Thus, $\mathrm{Re}[k_1]$ and $\mathrm{Re}[\bar{k}_1]$ have the same sign as that of λ_1 (which is real) for $\mathrm{d}E/\mathrm{d}v < 0$.

For $n = 4$, (B15) become

$$\left[(v^2 - c^2)\frac{\partial^2}{\partial X_1^2} - 2v\lambda_1\frac{\partial}{\partial X_1} + \lambda_1^2 + c^2\right](\rho\hat{\phi}_{UF}^{(2)} - \hat{\phi}_{LF}^{(2)})$$
$$= 2\left[-(v^2 - c^2)\frac{\partial^2}{\partial X_1 \partial X_2} + v\left(\lambda_1\frac{\partial}{\partial X_2} + \lambda_2\frac{\partial}{\partial X_1}\right) - \lambda_1\lambda_2\right](\rho\hat{\phi}_{UF}^{(1)} - \hat{\phi}_{LF}^{(1)}), \tag{B 20a}$$

$$\left(\frac{\partial^2}{\partial X_1^2} - 1\right)(D\hat{\phi}_{UF}^{(2)} + \hat{\phi}_{LF}^{(2)}) = -2\frac{\partial^2(D\hat{\phi}_{UF}^{(1)} + \hat{\phi}_{LF}^{(1)})}{\partial X_1 \partial X_2}. \tag{B 20b}$$

For $(\hat{\phi}_{UF}^{(2)}, \hat{\phi}_{LF}^{(2)})$ to have a solution that is not secular in X_1, the inhomogeneous terms on the right-hand sides of (B20) must vanish, and we have

$$q = q_\pm \exp(k_2 X_2), \quad \bar{q} = \bar{q}_\pm \exp(\bar{k}_2 X_2), \tag{B21a,b}$$

$$r = r_\pm, \quad \bar{r} = \bar{r}_\pm, \tag{B21c,d}$$

where q_+, $\bar{q}_+$, r_+, and $\bar{r}_+$ are undetermined constants for $X_1, X_2 > 0$, and q_-, $\bar{q}_-$, r_-, and $\bar{r}_-$ are those for $X_1, X_2 < 0$. The k_2 and $\bar{k}_2$ are the following given constants:

$$k_2 = \frac{v + c/\beta}{v^2 - c^2}\lambda_2, \quad \bar{k}_2 = \frac{v - c/\beta}{v^2 - c^2}\lambda_2, \tag{B22a,b}$$

where the coefficients $(v + c/\beta)/(v^2 - c^2)$ and $(v - c/\beta)/(v^2 - c^2)$ are positive when $\mathrm{d}E/\mathrm{d}v > 0$, since $v > c$ (see (2.20)) and $\beta > 1$. Thus, $\mathrm{Re}[k_2]$ and $\mathrm{Re}[\bar{k}_2]$ have the same sign as that of $\mathrm{Re}[\lambda_2]$ for $\mathrm{d}E/\mathrm{d}v > 0$.

Appendix C. Matching of the core solution and the far-field solution

Let us connect the core solution $(\hat{\phi}_{UC}, \hat{\phi}_{LC}, \hat{\eta}_C)$ obtained in § 3 and the far-field solution $(\hat{\phi}_{UF}, \hat{\phi}_{LF}, \hat{\eta}_F)$ obtained in Appendix B. In the core region, the far-field solution $(\hat{\phi}_{UF}^{(n)}, \hat{\phi}_{LF}^{(n)}, \hat{\eta}_F^{(n)})$ is expanded in power series of X_1 (or εx) and X_2 (or $\varepsilon^2 x$):

$$\hat{h}_F^{(n)} = (\hat{h}_F^{(n)})_0 + \varepsilon x\left(\frac{\partial\hat{h}_F^{(n)}}{\partial X_1}\right)_0 + \varepsilon^2\left[\frac{x^2}{2}\left(\frac{\partial^2\hat{h}_F^{(n)}}{\partial X_1^2}\right)_0 + x\left(\frac{\partial\hat{h}_F^{(n)}}{\partial X_2}\right)_0\right] + \cdots, \tag{C 1}$$

https://doi.org/10.1017/S0022112008002802 Published online by Cambridge University Press

where $\hat{h}$ represents $(\hat{\phi}_U, \hat{\phi}_L, \hat{\eta})$, and the quantities in the parentheses with a subscript 0 are evaluated at $X_1 = X_2 = 0$. With this reordering, we collect the same orders of ε, and have a reordered form (say, $(\hat{\phi}^{(n)*}_{UF}, \hat{\phi}^{(n)*}_{LF}, \hat{\eta}^{(n)*}_{F})$) of $(\hat{\phi}^{(n)}_{UF}, \hat{\phi}^{(n)}_{LF}, \hat{\eta}^{(n)}_{F})$. We then compare the forms of the two solutions $(\hat{\phi}^{(n)}_{UC}, \hat{\phi}^{(n)}_{LC}, \hat{\eta}^{(n)}_{C})$ and $(\hat{\phi}^{(n)*}_{UF}, \hat{\phi}^{(n)*}_{LF}, \hat{\eta}^{(n)*}_{F})$ at each n and match them from $n = 1$. The matching is accomplished if the conditions

$$\left[\hat{\phi}^{(n)}_{UC}\right]_{x\to\pm\infty} = \hat{\phi}^{(n)*}_{UF}, \quad \left[\hat{\phi}^{(n)}_{LC}\right]_{x\to\pm\infty} = \hat{\phi}^{(n)*}_{LF}, \quad \left[\hat{\eta}^{(n)}_{C}\right]_{x\to\pm\infty} = \hat{\eta}^{(n)*}_{F}, \tag{C 2}$$

are satisfied.

For $n = 1$, since $\hat{\phi}^{(1)*}_{UF} = (\hat{\phi}^{(1)}_{UF})_0$ and $\hat{\phi}^{(1)*}_{LF} = (\hat{\phi}^{(1)}_{LF})_0$, the matching is accomplished if

$$\left[\hat{\phi}^{(1)}_{UC}\right]_{x\to\pm\infty} = -\frac{q_\pm + \bar{q}_\pm}{D} + r_\pm + \bar{r}_\pm, \quad \left[\hat{\phi}^{(1)}_{LC}\right]_{x\to\pm\infty} = q_\pm + \bar{q}_\pm + \rho(r_\pm + \bar{r}_\pm), \tag{C3a,b}$$

where (B17a, b) with (B21) are used, and both upper or both lower signs should be chosen in the double signs.

For $n = 2$, since $\hat{\phi}^{(2)*}_{UF} = (\hat{\phi}^{(2)}_{UF})_0 + x(\partial\hat{\phi}^{(1)}_{UF}/\partial X_1)_0$ and $\hat{\phi}^{(2)*}_{LF} = (\hat{\phi}^{(2)}_{LF})_0 + x(\partial\hat{\phi}^{(1)}_{LF}/\partial X_1)_0$, two different kinds of terms, i.e. those independent of x and those proportional to x, are included in the matching conditions for $\hat{\phi}_U$ and $\hat{\phi}_L$. The relations among those proportional to x contribute to a determination of the unknowns at this order. It is convenient to represent them in terms of $\hat{u}^{(2)}_{UC}$ and $\hat{u}^{(2)}_{LC}$ defined by (3.20), i.e.

$$\left[\hat{u}^{(2)}_{UC}\right]_{x\to\pm\infty} = \frac{\beta\lambda_1}{c}(-q_\pm + \bar{q}_\pm) - D(r_\pm - \bar{r}_\pm), \tag{C 4a}$$

$$\left[\hat{u}^{(2)}_{LC}\right]_{x\to\pm\infty} = \frac{\beta\lambda_1}{c}(-q_\pm + \bar{q}_\pm) + \rho(r_\pm - \bar{r}_\pm), \tag{C 4b}$$

where (B17) with (B21) are used, and both upper or both lower signs should be chosen in the double signs. The matching conditions for $\hat{\eta}$ are automatically satisfied if (C3) and (C4) are satisfied.

Moreover, from the boundary conditions (2.36) and the fact that $\mathrm{Re}[k_1]$ and $\mathrm{Re}[\bar{k}_1]$ in (B17a, b) have the same sign as that of λ_1 (which is real) for $\mathrm{d}E/\mathrm{d}v < 0$ (see the statement after (B19)), and $\mathrm{Re}[k_2]$ and $\mathrm{Re}[\bar{k}_2]$ have the same sign as that of $\mathrm{Re}[\lambda_2]$ for $\mathrm{d}E/\mathrm{d}v > 0$ (see the statement after (B22)), we have

$$q_+ = \bar{q}_+ = r_+ = \bar{r}_- = 0 \quad \text{when} \quad \lambda_1 > 0, \tag{C 5a}$$

$$q_- = \bar{q}_- = r_+ = \bar{r}_- = 0 \quad \text{when} \quad \lambda_1 < 0, \tag{C 5b}$$

for $\mathrm{d}E/\mathrm{d}v < 0$, and

$$q_+ = \bar{q}_+ = r_+ = \bar{r}_- = 0 \quad \text{when} \quad \mathrm{Re}[\lambda_2] > 0, \tag{C5c}$$

$$q_- = \bar{q}_- = r_+ = \bar{r}_- = 0 \quad \text{when} \quad \mathrm{Re}[\lambda_2] < 0, \tag{C5d}$$

for $\mathrm{d}E/\mathrm{d}v > 0$. The twelve undetermined constants $[\hat{\phi}^{(1)}_{UC}]_{x\to\infty}$, $[\hat{\phi}^{(1)}_{LC}]_{x\to\infty}$, $[\hat{u}^{(2)}_{UC}]_{x\to\infty}$, $[\hat{u}^{(2)}_{LC}]_{x\to\infty}$, $q_\pm$, $\bar{q}_\pm$, $r_\pm$, and $\bar{r}_\pm$ (note that $[\hat{\phi}^{(1)}_{UC}]_{x\to-\infty}$, $[\hat{\phi}^{(1)}_{LC}]_{x\to-\infty}$, $[\hat{u}^{(2)}_{UC}]_{x\to-\infty}$, and $[\hat{u}^{(2)}_{LC}]_{x\to-\infty}$ are given by (3.21)) are determined by the twelve equations (C3)–(C5). We have

$$\rho\left[\hat{\phi}^{(1)}_{UC}\right]_{x\to\infty} = \left[\hat{\phi}^{(1)}_{LC}\right]_{x\to\infty} = \frac{\rho}{D}\left[\hat{u}^{(2)}_{UC}\right]_{x\to\infty} = -\left[\hat{u}^{(2)}_{LC}\right]_{x\to\infty} = \frac{\lambda_1}{\rho + D}\frac{\mathrm{d}}{\mathrm{d}v}\left(\frac{T_U + \rho T_L}{v}\right), \tag{C6a–d}$$

$$q_+ = \bar{q}_+ = r_+ = \bar{r}_- = 0, \tag{C6e}$$

https://doi.org/10.1017/S0022112008002802 Published online by Cambridge University Press

$$q_- = \frac{c}{2\beta}\left(\frac{vM}{\lambda_1} + \lambda_1 \frac{\mathrm{d}M}{\mathrm{d}v}\right) - \frac{c^2\lambda_1}{2(1-\rho)}\frac{\mathrm{d}\Omega}{\mathrm{d}v}, \tag{C6f}$$

$$\bar{q}_- = -\frac{c}{2\beta}\left(\frac{vM}{\lambda_1} + \lambda_1 \frac{\mathrm{d}M}{\mathrm{d}v}\right) - \frac{c^2\lambda_1}{2(1-\rho)}\frac{\mathrm{d}\Omega}{\mathrm{d}v}, \tag{C6g}$$

$$r_- = -\bar{r}_+ = -\frac{\lambda_1}{\rho + D}\frac{\mathrm{d}}{\mathrm{d}v}\left(\frac{T_U/\rho + T_L}{v}\right), \tag{C6h}$$

when $\lambda_1 > 0$ and $\mathrm{d}E/\mathrm{d}v < 0$ or $\mathrm{Re}[\lambda_2] > 0$ and $\mathrm{d}E/\mathrm{d}v > 0$, and

$$\left[\hat{\phi}^{(1)}_{UC}\right]_{x\to\infty} = \frac{\lambda_1}{\rho + D}\frac{\mathrm{d}}{\mathrm{d}v}\left(-\Omega + \frac{T_U/\rho + T_L}{v}\right), \tag{C 7a}$$

$$\left[\hat{\phi}^{(1)}_{LC}\right]_{x\to\infty} = \frac{\lambda_1}{\rho + D}\frac{\mathrm{d}}{\mathrm{d}v}\left(D\Omega + \frac{T_U + \rho T_L}{v}\right), \tag{C 7b}$$

$$\left[\hat{u}^{(2)}_{UC}\right]_{x\to\infty} = vM + \lambda_1^2\frac{\mathrm{d}M}{\mathrm{d}v} + \frac{D\lambda_1}{\rho + D}\frac{\mathrm{d}}{\mathrm{d}v}\left(\frac{T_U/\rho + T_L}{v}\right), \tag{C 7c}$$

$$\left[\hat{u}^{(2)}_{LC}\right]_{x\to\infty} = vM + \lambda_1^2\frac{\mathrm{d}M}{\mathrm{d}v} - \frac{\lambda_1}{\rho + D}\frac{\mathrm{d}}{\mathrm{d}v}\left(\frac{T_U + \rho T_L}{v}\right), \tag{C 7d}$$

$$q_- = \bar{q}_- = r_+ = \bar{r}_- = 0, \tag{C 7e}$$

$$q_+ = -\frac{c}{2\beta}\left(\frac{vM}{\lambda_1} + \lambda_1 \frac{\mathrm{d}M}{\mathrm{d}v}\right) + \frac{c^2\lambda_1}{2(1-\rho)}\frac{\mathrm{d}\Omega}{\mathrm{d}v}, \tag{C 7f}$$

$$\bar{q}_+ = \frac{c}{2\beta}\left(\frac{vM}{\lambda_1} + \lambda_1 \frac{\mathrm{d}M}{\mathrm{d}v}\right) + \frac{c^2\lambda_1}{2(1-\rho)}\frac{\mathrm{d}\Omega}{\mathrm{d}v}, \tag{C 7g}$$

$$r_- = -\bar{r}_+ = -\frac{\lambda_1}{\rho + D}\frac{\mathrm{d}}{\mathrm{d}v}\left(\frac{T_U/\rho + T_L}{v}\right), \tag{C 7h}$$

when $\lambda_1 < 0$ and $\mathrm{d}E/\mathrm{d}v < 0$ or $\mathrm{Re}[\lambda_2] < 0$ and $\mathrm{d}E/\mathrm{d}v > 0$. Note that E, Ω, M, T_U, and T_L are defined by (2.26) and (2.28).

Appendix D. Small-amplitude limit

The Kadomtsev–Petviashvili (KP) equation with negative dispersion (Kadomtsev & Petviashvili 1970) is often used for analysing the three-dimensional motion of small-amplitude long waves in a two-layer fluid. The KP equation is derived systematically from the set of Euler equations (2.1)–(2.7) by assuming small amplitude and long waves. Specifically, the following scalings for the variables in the Euler set:

$$\frac{\partial}{\partial y} = O(\delta^2), \quad \frac{\partial}{\partial z} = O(1), \quad \frac{\partial}{\partial t} = O(\delta^3), \tag{D 1a}$$

$$\frac{\partial}{\partial x} = O(\delta), \quad \eta = O(\delta^2), \quad \frac{\partial \phi_v}{\partial x} = -v + O(\delta^2), \quad \frac{\partial \phi_L}{\partial x} = -v + O(\delta^2), \tag{D 1b}$$

for small δ with

$$v_s \equiv v - c = O(\delta^2) \tag{D 2}$$

https://doi.org/10.1017/S0022112008002802 Published online by Cambridge University Press

(c is defined by (2.21)), lead to the KP equation with negative dispersion:

$$\frac{\partial}{\partial x}\left[\frac{\partial \eta}{\partial t}-v_s\frac{\partial \eta}{\partial x}+\alpha_1\frac{\partial}{\partial x}\left(\frac{\eta^2}{2}\right)+\alpha_2\frac{\partial^3\eta}{\partial x^3}\right]+\frac{c}{2}\frac{\partial^2\eta}{\partial y^2}=0, \tag{D 3}$$

where

$$\alpha_1=-\frac{3c}{2D}\frac{\rho-D^2}{\rho+D},\quad \alpha_2=\frac{cD}{6}\frac{\rho D+1}{\rho+D}(>0) \tag{D 4}$$

(see Craig, Guyenne & Kalisch (2005) for a derivation using Hamiltonian formulation). The velocity potentials ϕ_U and ϕ_L are related to η by

$$-\frac{D}{c}\left(\frac{\partial \phi_U}{\partial x}+v\right)=\frac{1}{c}\left(\frac{\partial \phi_L}{\partial x}+v\right)=\eta. \tag{D 5}$$

The KP equation (D3) has the following solitary wave solution for $v_s>0$:

$$\eta=\eta_s(x)\equiv\frac{3v_s}{\alpha_1}\mathrm{sech}^2\left(\sqrt{\frac{v_s}{\alpha_2}}\frac{x}{2}\right). \tag{D 6}$$

To examine the linear stability of this small-amplitude solitary wave (D6) with respect to transverse disturbances, we put

$$\eta=\eta_s(x)+\hat{\eta}(x)\exp(\lambda t+\mathrm{i}\varepsilon y), \tag{D 7}$$

where ε is a given positive constant and λ is a complex constant to be determined. Substituting (D7) into (D3) and linearizing with respect to $\hat{\eta}$, we have

$$\frac{\mathrm{d}}{\mathrm{d}x}\left[\lambda\hat{\eta}-v_s\frac{\mathrm{d}\hat{\eta}}{\mathrm{d}x}+\alpha_1\frac{\mathrm{d}}{\mathrm{d}x}(\eta_s\hat{\eta})+\alpha_2\frac{\mathrm{d}^3\hat{\eta}}{\mathrm{d}x^3}\right]-\frac{c}{2}\varepsilon^2\hat{\eta}=0. \tag{D 8}$$

This equation (D8) together with a decaying condition

$$\hat{\eta}(x)\to 0\quad\text{as}\quad x\to\pm\infty, \tag{D 9}$$

constitutes an eigenvalue problem for $\hat{\eta}$ with eigenvalue λ. We can make an asymptotic analysis of this system (D8) and (D9) for small ε in the same way as described in Kataoka & Tsutahara (2004*b*). They sought a solution of (D8) and (D9) where the η_s of the third term on the left-hand side of (D8) is replaced by a general function of η_s (say $f(\eta_s)$). In their paper the analysis for $\mathrm{d}P/\mathrm{d}v_s>0$ with

$$P(v_s)=\frac{1}{2}\int_{-\infty}^{\infty}\eta_s^2\,\mathrm{d}x, \tag{D 10}$$

was given, but that for $\mathrm{d}P/\mathrm{d}v_s<0$ can be made in a similar way, so that the reader is referred to that paper for the analytical process. Here only the results are presented for both cases. The asymptotic solution of (D8) and (D9) for small ε is expressed in power series of ε as (3.2), (3.3*c*), (B2*c*), and their components are given as follows:

https://doi.org/10.1017/S0022112008002802 Published online by Cambridge University Press

The λ_1 and λ_2 are

$$\lambda_1 = \begin{cases} \pm\sqrt{\dfrac{-cP}{\mathrm{d}P/\mathrm{d}v_s}} & \text{for } \dfrac{\mathrm{d}P}{\mathrm{d}v_s} < 0, \\ \pm \mathrm{i}\sqrt{\dfrac{cP}{\mathrm{d}P/\mathrm{d}v_s}} & \text{for } \dfrac{\mathrm{d}P}{\mathrm{d}v_s} > 0, \end{cases} \qquad \lambda_2 = \begin{cases} -\dfrac{\lambda_1}{|\lambda_1|} Q_s & \text{for } \dfrac{\mathrm{d}P}{\mathrm{d}v_s} < 0, \\ \begin{cases} \pm Q_s & \text{if } Q_s < 0, \\ \text{no solution} & \text{if } Q_s > 0, \end{cases} & \text{for } \dfrac{\mathrm{d}P}{\mathrm{d}v_s} > 0, \end{cases} \tag{D11a,b}$$

where P is defined by (D10) and

$$Q_s(v_s) = -\frac{cP}{4(\mathrm{d}P/\mathrm{d}v_s)^2}\left(\frac{\mathrm{d}M}{\mathrm{d}v_s} - \frac{M}{P}\frac{\mathrm{d}P}{\mathrm{d}v_s}\right)\frac{\mathrm{d}M}{\mathrm{d}v_s}, \quad M(v_s) = \int_{-\infty}^{\infty} \eta_s \,\mathrm{d}x. \tag{D12a,b}$$

The $\hat{\eta}_C^{(0)}$, $\hat{\eta}_C^{(1)}$ (core solution), and $\hat{\eta}_F^{(2)}$ (far-field solution) are

$$\hat{\eta}_C^{(0)} = \frac{\mathrm{d}\eta_s}{\mathrm{d}x}, \quad \hat{\eta}_C^{(1)} = -\lambda_1 \frac{\partial \eta_s}{\partial v_s}, \tag{D13a,b}$$

$$\hat{\eta}_F^{(2)} = \frac{k_{1s}}{c} q_{s\pm} \exp(k_{1s}X_1 + k_{2s}X_2) + \frac{\bar{k}_{1s}}{c}\bar{q}_{s\pm}\exp(\bar{k}_{1s}X_1 + \bar{k}_{2s}X_2), \tag{D13c}$$

where X_1 and X_2 are defined by (B1), and k_{1s}, $\bar{k}_{1s}$, k_{2s}, $\bar{k}_{2s}$ are the following given constants:

$$k_{1s} = \frac{\lambda_1}{2v_s}(1+\beta_s), \quad \bar{k}_{1s} = \frac{\lambda_1}{2v_s}(1-\beta_s), \quad k_{2s} = \frac{\lambda_2}{2v_s}\left(1+\frac{1}{\beta_s}\right), \quad \bar{k}_{2s} = \frac{\lambda_2}{2v_s}\left(1-\frac{1}{\beta_s}\right), \tag{D 14}$$

with

$$\beta_s = \begin{cases} \mathrm{i}\sqrt{-\left(1+\dfrac{2v_s}{P}\dfrac{\mathrm{d}P}{\mathrm{d}v_s}\right)} & \text{for } \dfrac{\mathrm{d}P}{\mathrm{d}v_s} < -\dfrac{P}{2v_s}, \\ \sqrt{1+\dfrac{2v_s}{P}\dfrac{\mathrm{d}P}{\mathrm{d}v_s}} & \text{for } \dfrac{\mathrm{d}P}{\mathrm{d}v_s} > -\dfrac{P}{2v_s}. \end{cases} \tag{D 15}$$

In (D13c), q_{s+} and $\bar{q}_{s+}$ are coefficients for $X_1, X_2 > 0$, while q_{s-} and $\bar{q}_{s-}$ are those for $X_1, X_2 < 0$, and specifically given by

$$q_{s+} = \bar{q}_{s+} = 0, \quad q_{s-} = \frac{c}{\beta_s}\left(k_{1s}v_s\frac{\mathrm{d}M}{\mathrm{d}v_s} + \frac{cM}{2\lambda_1}\right), \quad \bar{q}_{s-} = -\frac{c}{\beta_s}\left(\bar{k}_{1s}v_s\frac{\mathrm{d}M}{\mathrm{d}v_s} + \frac{cM}{2\lambda_1}\right), \tag{D 16}$$

when $\lambda_1 > 0$ and $\mathrm{d}P/\mathrm{d}v_s < 0$ or $\lambda_2 > 0$ and $\mathrm{d}P/\mathrm{d}v_s > 0$, while

$$q_{s+} = -\frac{c}{\beta_s}\left(k_{1s}v_s\frac{\mathrm{d}M}{\mathrm{d}v_s} + \frac{cM}{2\lambda_1}\right), \quad \bar{q}_{s+} = \frac{c}{\beta_s}\left(\bar{k}_{1s}v_s\frac{\mathrm{d}M}{\mathrm{d}v_s} + \frac{cM}{2\lambda_1}\right), \quad q_{s-} = \bar{q}_{s-} = 0, \tag{D 17}$$

when $\lambda_1 < 0$ and $\mathrm{d}P/\mathrm{d}v_s < 0$ or $\lambda_2 < 0$ and $\mathrm{d}P/\mathrm{d}v_s > 0$.

From (D11), there is a solution for which λ has a positive real part if $\mathrm{d}P/\mathrm{d}v_s < 0$ or $Q_s < 0$. Thus, a sufficient condition for the transverse instability of a small-amplitude solitary wave is

$$\frac{\mathrm{d}P}{\mathrm{d}v_s} < 0 \quad \text{or} \quad Q_s < 0. \tag{D 18}$$

https://doi.org/10.1017/S0022112008002802 Published online by Cambridge University Press

The solution (D6) never satisfies the condition (D18), which is consistent with the stability results shown in § 4. In fact, the above criterion (D18) and the asymptotic solution (λ given by (D11), the core solution given by (D13a, b), and the far-field solution given by (D13c)) of the KP equation can be derived directly from the criterion (3.24) and the asymptotic solution (λ given by (3.18) and (3.22), the core solution given by (3.1) and (3.14), and the far-field solution given by (B17c)) of the Euler set only by applying the scalings (D1b) and (D2) ((D1a) are not used) and keeping the leading-order terms in δ of each component. In that process, note that $v - c \to v_s = O(\delta^2)$, $\mathrm{d}/\mathrm{d}v \to \mathrm{d}/\mathrm{d}v_s = O(\delta^{-2})$, $E \to 2(1-\rho)P = O(\delta^3)$, $M = O(\delta)$, $T_U = O(\delta^3)$, $T_L = O(\delta^3)$, $\mathrm{d}\Omega/\mathrm{d}v \to -c(1+\rho/D)\mathrm{d}M/\mathrm{d}v_s$, $k_1 \to k_{1s}$, $k_2 \to k_{2s}$, $\beta \to \beta_s$, $q_\pm \to q_{s\pm}$, and $\bar{q}_\pm \to \bar{q}_{s\pm}$ as $\delta \to 0$.

REFERENCES

Amick, C. J. & Turner, R. E. L. 1986 A global theory of internal solitary waves in two-fluid systems. *Trans. Am. Math. Soc.* **298**, 431–484.

Benjamin, T. B. 1967 Internal waves of permanent form in fluids of great depth. *J. Fluid Mech.* **29**, 559–592.

Benjamin, T. B. 1972 The stability of solitary waves. *Proc. R. Soc. Lond.* A **328**, 153–183.

Calvo, D. C. & Akylas, T. R. 2003 On interfacial gravity–capillary solitary waves of the Benjamin type and their stability. *Phys. Fluids* **15**, 1261–1270.

Craig, W., Guyenne, P. & Kalisch, H. 2005 Hamiltonian long-wave expansions for free surfaces and interfaces. *Commun. Pure Appl. Maths* **68**, 1587–1641.

Davis, R. E. & Acrivos, A. 1967 Solitary internal waves in deep water. *J. Fluid Mech.* **29**, 593–607.

Dias, F. & Vanden-Broeck, J.-M. 2003 On internal fronts. *J. Fluid Mech.* **479**, 145–154.

Evans, W. A. B. & Ford, M. J. 1996 An integral equation approach to internal (2-layer) solitary waves. *Phys. Fluids* **8**, 2032–2047.

Funakoshi, M. & Oikawa, M. 1986 Long internal waves of large-amplitude in a two-layer fluid. *J. Phys. Soc. Japan* **55**, 128–144.

Grue, J., Jensen, A., Rusås, P. O. & Sveen, J. K. 1999 Properties of large amplitude internal waves. *J. Fluid Mech.* **380**, 257–278.

Jeffery, A. & Kakutani, T. 1970 Stability of the Burgers shock wave and the Korteweg–de Vries soliton. *Indiana Univ. Math. J.* **20**, 463–468.

Kadomtsev, B. B. & Petviashvili, V. I. 1970 On the stability of solitary waves in a weakly dispersing medium. *Sov. Phys. Dokl.* **15**, 539–541.

Kakutani, T. & Yamasaki, N. 1978 Solitary waves on a two-layer fluid. *J. Phys. Soc. Japan* **45**, 674–679.

Kataoka, T. 2006 The stability of finite-amplitude interfacial solitary waves. *Fluid Dyn. Res.* **38**, 831–867.

Kataoka, T. & Tsutahara, M. 2004*a* Transverse instability of surface solitary waves. *J. Fluid Mech.* **512**, 211–221.

Kataoka, T. & Tsutahara, M. 2004*b* Instability of solitary wave solutions to long-wavelength transverse perturbations in the generalized Kadomtsev–Petviashvili equation with negative dispersion. *Phys. Rev.* E **70**, 016604.

Kivshar, Y. S. & Pelinovsky, D. E. 2000 Self-focusing and transverse instabilities of solitary waves. *Phys. Rep.* **331**, 117–195.

Laget, O. & Dias, F. 1997 Numerical computation of capillary–gravity interfacial solitary waves. *J. Fluid Mech.* **349**, 221–251.

Longuet-Higgins, M. S. & Tanaka, M. 1997 On the crest instabilities of steep surface waves. *J. Fluid Mech.* **336**, 51–68.

Meiron, D. I. & Saffman, P. G. 1983 Overhanging interfacial gravity waves of large amplitude. *J. Fluid Mech.* **129**, 213–218.

Michallet, H. & Barthélemy, E. 1998 Experimental study of interfacial solitary waves. *J. Fluid Mech.* **366**, 159–177.

https://doi.org/10.1017/S0022112008002802 Published online by Cambridge University Press

Ostrovsky, L. A. & Shrira, V. I. 1976 Instability and self-refraction of solitons. *Sov. Phys. JETP* **44**, 738–743.

Pullin, D. I. & Grimshaw, R. H. J. 1988 Finite-amplitude solitary waves at the interface between two homogeneous fluids. *Phys. Fluids* **31**, 3550–3559.

Rusås, P. O. & Grue, J. 2002 Solitary waves and conjugate flows in a three-layer fluid. *Eur. J. Mech.* B/*Fluids* **21**, 185–206.

Sha, H. & Vanden-Broeck, J.-M. 1993 Two-layer flows past a semicircular obstruction. *Phys. Fluids* A **5**, 2661–2668.

Shrira, V. I. 1980 Nonlinear refraction of solitons. *Sov. Phys. JETP* **52**, 44–49.

Tanaka, M. 1986 The stability of solitary waves. *Phys. Fluids* **29**, 650–655.

Tanaka, M., Dold, J. W., Lewy, M. & Peregrine, D. H. 1987 Instability and breaking of a solitary wave. *J. Fluid Mech.* **185**, 235–248.

Turner, R. E. L. & Vanden-Broeck, J.-M. 1988 Broadening of interfacial solitary waves. *Phys. Fluids* **31**, 2486–2490.

Zakharov, V. E. 1975 Instability and nonlinear oscillations of solitons. *JETP Lett.* **22**, 172–173.

https://doi.org/10.1017/S0022112008002802 Published online by Cambridge University Press